The Canadian Mineralogist
Vol. 39, pp. 607-637 (2001)

THE STRUCTURE OF THE LUKKULAISVAARA INTRUSION, OULANKA GROUP, NORTHERN KARELIA: PETROLOGICAL IMPLICATIONS

VIKTOR A. GLEBOVITSKY[§], VLADIMIR S. SEMENOV AND BORIS V. BELYATSKY

Institute of Precambrian Geology and Geochronology, Russian Academy of Sciences,
Makarova Emb. 2, St. Petersburg 199034, Russia

EUGENE V. KOPTEV-DVORNIKOV[¶], NINA F. PCHELINTSEVA AND BORIS S. KIREEV

Department of Geology, Moscow State University, University Square, 1, Moscow 119899, Russia

ALEXANDER B. KOLTSOV

Department of Geology, St. Petersburg State University, Universitetskaja emb. 7/9, St. Petersburg 100034, Russia

ABSTRACT

The Lukkulaisvaara intrusion (U–Pb age: 2442 ± 1.9 Ma), in northern Karelia, Russia, belongs to the Oulanka plutonic group. The intrusion cuts rocks of the Archean granite – migmatite – gneiss basement and is disconformably overlain by Proterozoic metavolcanic rocks. The layered body does not exceed 4600 m in thickness; data obtained on the structural profile of the intrusion suggest a complete section. Its weighted-mean composition is equivalent to a magma of the marianite–boninite series, but whether or not this composition corresponds to the parental magma is uncertain owing to possible multiphase features of the intrusion. It is quite possible that large and small lenticular bodies of fine-grained gabbronorite whose texture suggests rapid crystallization are associated with injections of fresh magma. Crystallization to fine-grained gabbronorite in the process of magma chilling is related, in turn, to decompression. Chilling would be equally feasible in the case of the injection of residual melts, squeezed from lower horizons and already carrying cumulus minerals in the process of compaction. Structures in which fine-grained rocks occur do not differ from "potholes" in morphology and structural setting. Two genetic types of sulfides are distinguished: (a) sulfides of magmatic stage are present in fresh rocks, commonly with magmatic quartz and biotite; (b) a metasomatic sulfide assemblage contains the richest sulfide and platinum mineralization and is related to potholes. Amounts of sulfide in the metasomatic rocks are very variable (1–30 vol.%). Forty platinum-group minerals have been documented in sulfide-bearing metasomatic rocks; the concentration of noble metals (Pt + Pd) covers a wide range (0.3–10 ppm Pt, 0.42–66 ppm Pd). Sulfides in the cumulates and iron-bearing magmatic minerals altered by metasomatism are considered to be the source of the ore-bearing metasomatic assemblages. These assemblages were formed under the action of a reducing hydrothermal fluid. A high content of chlorine was observed in biotite (up to 0.55 wt%), amphibole (up to 2.5 wt%), chlorite (up to 0.1 wt%), and scapolite (up to 2.3 wt%). Examination of the metasomatic quartz reveals the presence of different types of micro-inclusions. Some are filled with liquid only, others are gas–liquid, aqueous – salt inclusions with a gas bubble, and hydrocarbon inclusions with various amounts of liquid. The highest T_h recorded is 370°C at a pressure of 1.5 kbar, as estimated using aqueous – salt inclusions. These data agree well with thermobarometric results calculated using estimated equilibration states. Nd and Sr isotopic data suggest that the metasomatic assemblages formed simultaneously with the layered intrusion (2442 Ma) during an autometasomatic process due to reworking of intrusive rocks by a mantle-derived fluid with an ε_{Nd} of +2.1 and an initial $^{87}Sr/^{86}Sr$ value of 0.7028.

Keywords: layered intrusion, structure, fine-grained bodies, mineralization, hydrothermal fluid, fluid inclusions, isotopic data, Lukkulaisvaara, Oulanka Group, Karelia, Russia.

SOMMAIRE

Le complexe intrusif de Lukkulaisvaara (age U–Pb: 2442 ± 1.9 Ma), dans la partie nord de la Karélie, en Russie, fait partie du groupe plutonique de Oulanka. Ce massif recoupe les roches archéennes (granite – migmatite – gneiss) du socle; il est recouvert par une suite métavolcanique d'âge protérozoïque. Le complexe stratiforme ne dépasse pas 4600 m en épaisseur; les données accumulées pour établir le profil structural font penser que la section est complète. La composition globale ajustée équivaudrait à un magma de la série marianite–boninite, mais il n'est pas assuré que cette composition représente le magma parental à cause

---

[§] *E-mail address*: gleb@ad.iggp.ras.spb.ru
[¶] *E-mail address*: ekoptev@geol.msu.ru

de la possibilité que la mise en place ait impliqué plus d'une épisode. Il est possible que la présence de lentilles de gabbronorite à grains fins et de taille variable soit due à une cristallisation rapide suite à l'injection de nouvelles venues de magma. La cristallisation d'un gabbronorite à grains fins est liée, à son tour, à une décompression. Une trempe serait également possible dans le cas d'injection d'un magma résiduel extrait d'un niveau inférieur par compression, et déjà porteur de minéraux cumulatifs en voie de compaction. Les structures dans lesquelles on trouve les roches à grains fins ne sont pas différentes des "nids de poule" en morphologie et contexte structural. Nous distinguons deux types génétiques de sulfures: (a) sulfures magmatiques, présents dans les roches saines, généralement avec quartz et biotite magmatiques, et (b) un assemblage de sulfures métasomatiques contenant les concentrations les plus élevées en sulfures et en platine, et lié à la formation des "nids de poule". Les proportions de sulfures dans les roches sujettes à une métasomatose sont très variables (1–30% par volume). Quarante minéraux du groupe du platine ont été documentés dans les roches métasomatisées à sulfures. La concentration en métaux nobles (Pt + Pd) varie aussi largement (0.3–10 ppm Pt, 0.42–66 ppm Pd). Les sulfures des cumulats et les minéraux magmatiques altérés par métasomatose seraient à l'origine des assemblages de sulfures métasomatiques. Ces assemblages se seraient formés en présence d'une phase fluide réductrice. Nous observons une teneur élevée en chlore dans la biotite (jusqu'à 0.55% en poids), l'amphibole (jusqu'à 2.5%), la chlorite (jusqu'à 0.1%), et la scapolite (jusqu'à 2.3%). Une étude du quartz métasomatique révèle la présence de différents types de micro-inclusions. Elles contiennent un liquide seulement dans certains cas, tandis que d'autres contiennent gaz + liquide, solution aqueuse avec inclusions de sel, avec une bulle gazeuse, et des inclusions d'hydrocarbures avec une proportion variable de liquide. La température d'homogénéisation maximale est de 370°C à une pression de 1.5 kbar, tel qu'estimée à partir des inclusions fluides avec inclusions de sel. Ces données concordent bien avec les résultats thermodynamiques calculées selon les ated using estimated equilibration states. Nd and Sr isotopic data suggest that the metasomatic assemblages formed simultaneously with the layered intrusion (2442 Ma) during an autometasomatic process due to reworking of intrusive rocks by a mantle-derived fluid with an ε_{Nd} of +2.1 and an initial $^{87}Sr/^{86}Sr$ value of 0.7028.

(Traduit par la Rédaction)

Mots-clés: complexe intrusif stratiforme, structure, venues à grains fins, minéralisation, fluide hydrothermal, inclusions fluides, données isotopiques, Lukkulaisvaara, Groupe d'Oulanka, Karélie, Russie.

INTRODUCTION

The layered intrusive complexes of northern Karelia are emplaced in Late Archean and Early Proterozoic volcanic and clastic terranes, at the boundary between the areas where the Archean and Proterozoic granitic rocks of the Baltic Shield occur (Fig. 1). According to recent geological data, the Archean basement, which is the oldest formation of the region (*ca*. 2.8 Ga), consists of granitic and tonalitic gneisses of the Karelian granite–greenstone terrane occurring in the southern part of the studied area. The block was rejuvenated *ca*. 1.8 Ga ago, and earlier gneisses of a similar type were recognized in the northeastern part of the area, which consists of the so-called Belomorian gneiss terrane. The Sumian–Sariolian metasedimentary and metavolcanic rocks (*ca*. 2.4 Ga) fill a trough (the Paanajarvi structure) developed within the Karelian granite–greenstone terrane. Yatulian metasediments (1.9–2.2 Ga) almost entirely cover the central part of the continental rift structure. Leucodiabase sills (*ca*. 2.05 Ga) were found within the sedimentary units. The following groups of granitic rocks were distinguished in the region: (1) Archean granite gneisses, (2) small bodies of younger granite rocks, mainly in the eastern and northeastern parts of the area, intruding the Archean granite gneisses, and (3) Svecofennian granites (1.7–1.8 Ga), forming large plutons in the northwestern part of the region. The Yatulian sedimentary and volcanic rocks and sills are associated with the Svecofennian granites, and occur as incompletely assimilated residues. The Kuoloyarvi unit of mafic and felsic volcanic rocks is believed to have been thrust over the Yatulian metasediments. Dykes of gabbro (2.4–2.5 Ga) and diabase (2.0–2.1 Ga) are predominant within the Archean basement.

Layered intrusions of northern Karelia are subdivided into two groups: Koilismaa, Finland (Alapieti 1982) and Oulanka, Russia (Shmygalev 1968, Lavrov 1971, Felitsin *et al.* 1989, Turchenko *et al.* 1991, Rudashevsky *et al.* 1991, Pchelintseva & Koptev-Dvornikov 1993, Klyunin *et al.* 1994, Semenov *et al.* 1995a, b, 1997, Barkov *et al.* 1996). Proterozoic deformation caused the Oulanka Group massifs to plunge to the northeast.

According to isotopic U–Pb and Sm–Nd geochemistry, the ages of massifs of the Oulanka group and associated volcanic rocks were determined as follows (Barkov *et al.* 1991, Turchenko 1992, Amelin *et al.* 1995, Amelin & Semenov 1996): 1) Lukkulaisvaara: 2442.1 ± 1.9 Ma (U–Pb method), 2) Kivakka: 2420 ± 23 Ma (Sm–Nd method), 2444.0 ± 1.0 Ma (U–Pb), Tsipringa: 2430 ± 26 Ma (Sm–Nd), 2441.3 ± 1.7 Ma (U–Pb), volcanic suites: 2442.0 ± 24.0 Ma (U–Pb).

It is remarkable that the Koilismaa intrusions, in Finland, have the same ages (Alapieti 1982). All the ages obtained by Sm–Nd and U–Pb methods are within analytical uncertainties, and do not allow us to discriminate among these intrusions.

In recent years, the Oulanka massifs were subject to detailed geological and geophysical work, including petrological and geochemical studies. These new results contribute significantly to our knowledge of the structure, genesis, and metallogeny of the massifs. In this

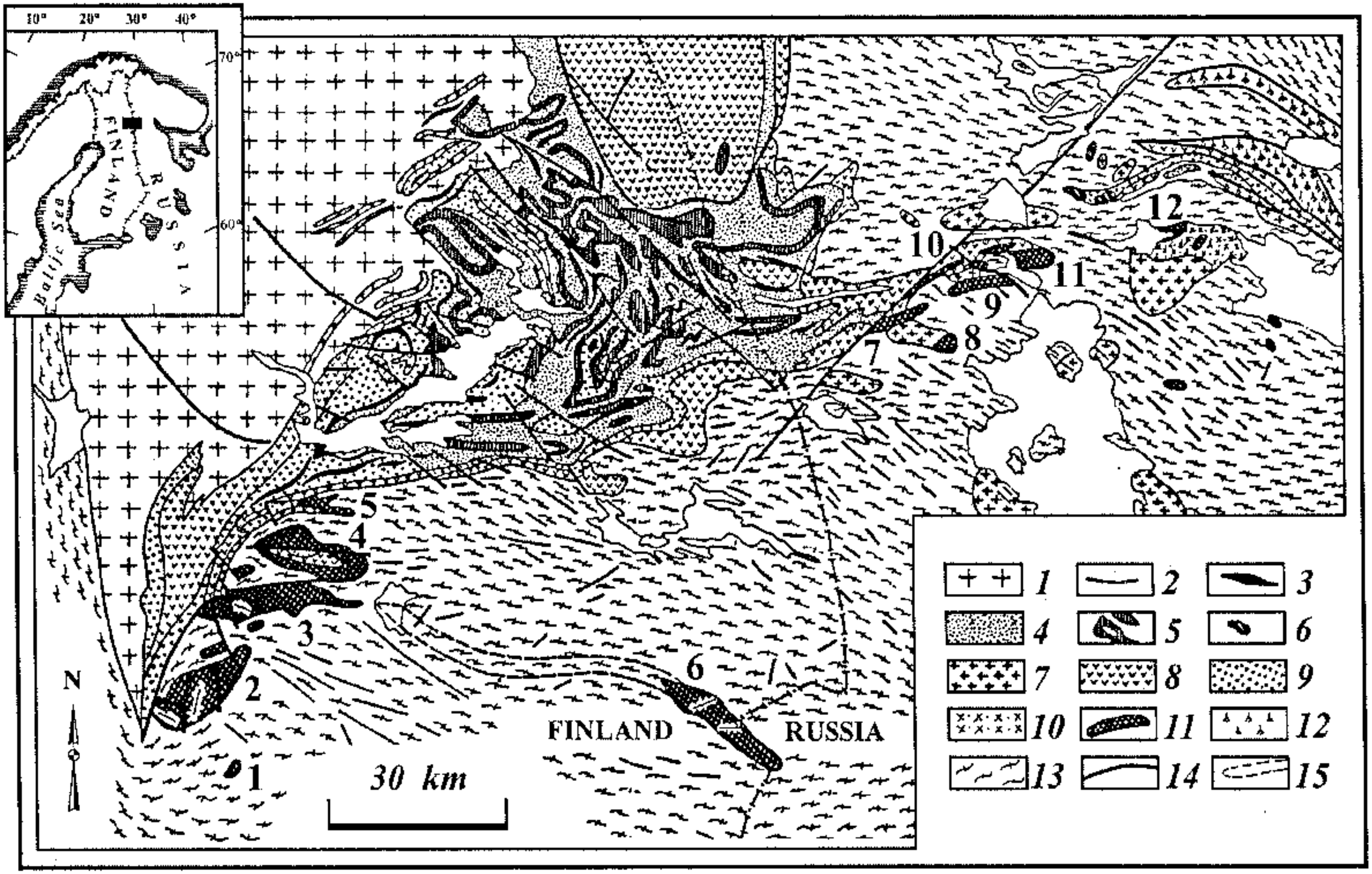

FIG. 1. Geological map of layered intrusions in northern Karelia, compiled after the data of Finnish geologists (geological map of northern Fennoscandia 1987; Gorbatschev *et al.* 1987, Alapieti 1982), Soviet state geological maps (1:200 000), and geophysical survey data. 1. Postorogenic granites (1.7–1.8 Ga); 2. Gabbro-diabase dykes (more than 1.9 Ga). Yatulian Group (1.9–2.2 Ga): 3. Leucodiabase sills, 4. Quartzites, phyllites, schists, and dolomites, 5. Basic volcanic rocks, 6. Serpentinites, 7. Monzodiorites and granites. Sumian–Sariolian Group (2.2–2.5 Ga): 8. Basic and acid volcanic rocks, 9. Quartzites and quartz–feldspar gneisses, 10. Diorites, 11. Layered intrusions (2.35–2.45 Ga). Archean basement: 12. Gneisses and amphibolite–greenstone belts (2.6–2.7), 13. Granite and tonalite gneisses. 14. Faults. 15. Outline of the Narankavaara massif projected to the Earth’s surface. Intrusions: (1) Pirivaara, (2) Syote, (3) Portivaara, (4) Kuusijarvi, (5) Kaukua, (6) Narankavaara, (7) Komettavaara, (8) Kivakka, (9) Tsipringa, (10) Njudamolaksha, (11) Lukkulaisvaara, and (12) Kundozerskii.

paper, we report the results of a study of the structure, geochemistry, and petrology of the Lukkulaisvaara intrusion, the relations of the alteration and ore minerals, including platinum-group minreals (PGM), the characteristics of fluid inclusions, P–T conditions of crystallization of the secondary minerals, and Sr and Nd isotope systematics of the altered assemblages.

METHODS

Geophysical survey data were used to prepare a geological map (Fig. 2). The maximum gradients in gravity correspond exactly to the boundaries of the bodies. This allowed precise mapping despite the generally poor exposure of the contact zones of the massifs. The depths of the bottoms of the massifs and the character of their vertical sections were established by special processing of data on gravity-field anomalies. Magnetic survey data demonstrated the internal structure of the massifs through the presence of primary ferromagnetic minerals (titanian magnetite and pyrrhotite).

To study the complex layering in detail, profiles were chosen in areas with maximum thickness and the most representative spectrum of rocks. The conditions of exposure of the Lukkulaisvaara intrusion did not allow us to characterize its vertical sequence in a single continuous section. Three profiles (1–1, 2–2 and 3–3) were used to describe the structure (Fig. 2). Profile 1–1 was reconstructed using data obtained from drill holes. Profiles 2–2 and 3–3 were obtained by surface mapping. To correlate the sequences along the 2–2 and 3–3 profiles, distinctive petrographic layers of leucocratic gabbronorites were used.

The rocks of Lukkulaisvaara generally have been significantly hydrothermally altered by postmagmatic processes, particularly in the upper part of the layered sequence and where the rocks are ore-bearing. Petrochemical data on the rocks modified under closed-system conditions are of particular value for rock identification. To distinguish the types of rocks, we used one of the variants of hierarchical cluster analysis (Ward 1963), which was tested for the classification of igne-

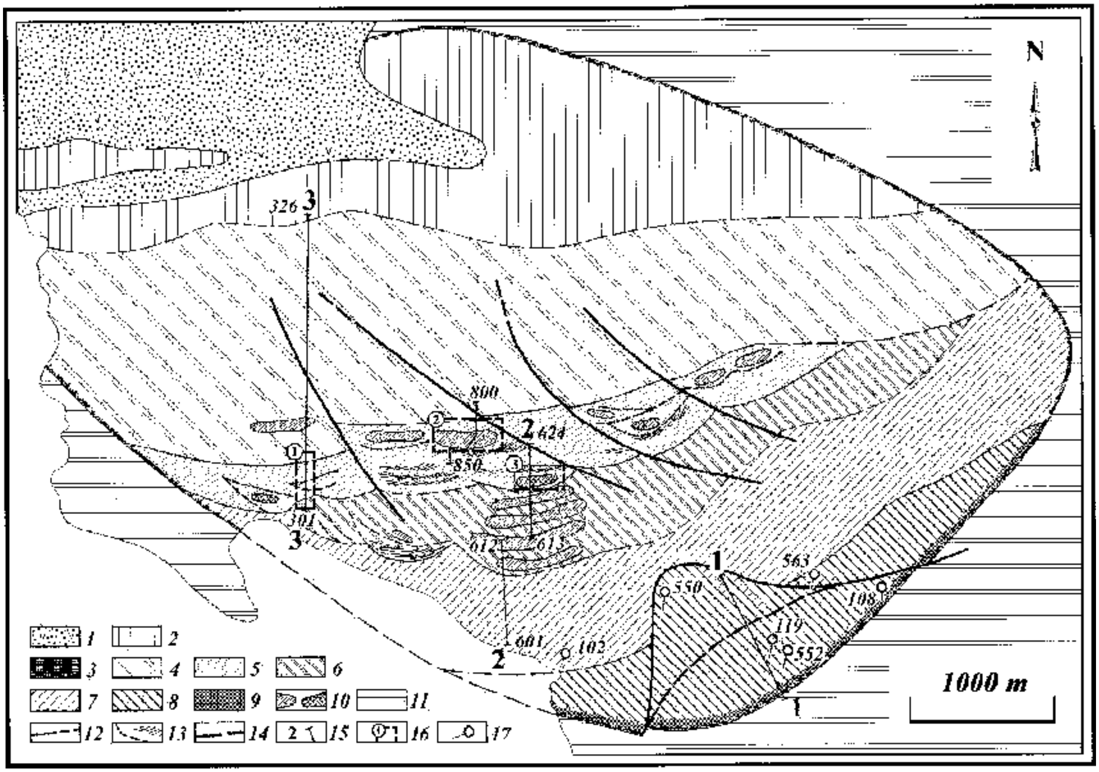

FIG. 2. Schematic geological map of the Lukkulaisvaara intrusion. 1. Metavolcanic rocks (2.4 Ga), 2. The upper boundary zone, composed of alternating norite and gabbronorite, 3. Gabbronorite-II zone, 4. Norite-II zone, 5. Gabbronorite-I zone, 6. Norite-I zone, 7. Ultrabasic zone, 8. Fine-grained rocks, 9. Granite gneisses and migmatites of the basement (2.6–2.7 Ga), 10. Geological boundaries; 11. Thin layers and boundaries of the potholes, 12. Faults, 13. Sampling profiles, 14. Location of detailed investigations.

ous rocks. This method was combined with the calculation of normative compositions of the rocks (in vol.%). The essence of this approach may be outlined as follows. A cluster may be characterized by the intragroup sum of squares, which is equal to the sum of squared distances of the cluster points to the average. To measure the distances, conventional Euclidean metrics were applied. Considering the intragroup sum of squares to be the target function, Ward (1963) combined two clusters that resulted in a minimal increase in the target function. Thus, according to Ward's method, the two most similar clusters are combined. Major-element analyses of 196 samples representing all of the main rock-types of the massif were processed this way. These data were used in a reconstruction of the integrated profile of the Lukkulaisvaara complex.

The major-element content of the rocks was determined by X-ray spectrometry and flame photometry (sodium) in the Central Research Group of the Physico-Chemical Studies of Minerals, Complex Expedition, All-Russian Institute of Mineral Resources, Narofominsk. The concentrations of Ni, Co, Cu, Cr, Zn, Ag, Au, Pt, Pd, Ru, Rh were measured by atomic absorption at the Department of Geochemistry, Faculty of Geology, Moscow State University. The samples were decomposed with hydrofluoric and perchloric acids and then analyzed in an air–acetylene flame with a Hitachi Atomic Absorption Spectrometer (model 207). The detection limits were 0.01 mg/mL for Cu and Cr, 0.03 mg/mL for Ni and Co, and 0.005 mg/mL for Zn. Analysis of the MO standard samples checked the accuracy of the determinations. Concentrations of La, Ce, Nd, Sm, Eu, Tb, Yb, and Lu were determined by instrumental neutron-activation analysis at Activation Laboratories Ltd, Ancaster, Ontario, Canada. The detection limits were: La 0.1 ppm, Ce 1.0 ppm, Nd 1.0 ppm, Sm 0.01 ppm, Eu 0.05 ppm, Tb 0.1 ppm, Yb 0.05 ppm, Lu 0.01 ppm.

The isotopic compositions of Sm, Nd, Rb, Sr were determined by isotope dilution with a precision not less than 1%. Chemical dissolution and separation of elements followed by mass-spectrometry analysis were carried out using ion-exchange and extraction according to the chromatographic techniques described by Richard *et al.* (1976). Isotope compositions of Sr and Nd were analyzed with an 8-collector Finnigan MAT–261 mass spectrometer (Laboratory of Isotope Geochronology and Geochemistry, Institute of Precambrian Geology and Geochronology, St. Petersburg) in a static regime. The Nd isotope composition was corrected for mass fractionation by normalization of determined values to the ratio $^{148}Nd/^{144}Nd = 0.24157$, and the determined Sr isotope composition was normalized to the ratio $^{88}Sr/^{86}Sr = 8.37521$. The Nd isotope ratio for the La Jolla standard was $^{143}Nd/^{144}Nd = 0.511883 \pm 7$ during the period of analytical procedure, and the Sr isotope ratio for SRM–987 standard $^{87}Sr/^{86}Sr = 0.710254 \pm 12$. Analytical blanks were 0.05, 0.01, 0.1 and 0.005 ng for Nd, Sm, Sr and Rb, respectively.

STRUCTURE OF THE LUKKULAISVAARA INTRUSION

The Lukkulaisvaara intrusion is located in the eastern part of the Paanajarvi rift structure, where it tapers off (Fig. 1). Drilling has shown an intrusive contact with the granite–gneiss basement. A series of weakly metamorphosed basalts, basaltic andesites, felsic volcanic rocks with a well-preserved amygdaloidal structure and with conglomerates (including gabbro pebbles from the intrusion) and greenstone in the lower part occurs on the eroded surface of the layered intrusion (Fig. 2). The volcanic rocks overlap the entire northwestern part of the intrusion, but some fragments of the intrusion are exposed on the surface within the volcanic sequence. Figure 2 gives a schematic geological map of the Lukkulaisvaara intrusion.

Geophysical (gravity and magnetic data) and geological relations suggest that the intrusion forms an irregular ellipse in plan; it has been traced along strike up to 10 km. The thickness of the intrusion, including those parts buried under Quaternary deposits, is up to 4.6 km; gravity surveys have shown it to be 1.5 km in depth and with a real thickness of about 4.5 km. The strike of layering and trachytic fabric is 0–15° ENE in the western and central parts, and 40–45° NE in the eastern part of the intrusion. The layering dips 45–70° to the N. An internal angular disconformity, marking a drastic change in the layering and orientation of the trachytic texture, was mapped in the southern part of the massif (Figs. 2, 3c). Within the layered complex, lenticular bodies of fine-grained gabbronorite and norite of variable thickness along the magmatic layering are identified (Figs. 2, 3). The presence of these bodies of gabbronorite and norite is a typical feature of the Lukkulaisvaara intrusion. Rocks called "pseudoconglomerates" mark the bottom zones of the lenticular bodies. "Pebbles", usually rounded, consist of fine-grained gabbronorite or coarse-grained pyroxenite and gabbronorite.

Low-angle eastward-plunging faults are well defined in the relief and locally traced by zones of schistosity. No significant displacements have been observed along them; this is supported by the results of magnetic surveys, in which the axes of magnetic anomalies are consistent with the strike of the layering. A thrust structure, marked in the ultrabasic zone of the layered series, is an exception. A block, made up of dunite and harzburgite and thrust over the mafic part of the section, was drilled here (Fig. 2). The gently pitching thrust-zone is represented by strongly schistose (mylonitic) rocks of ultrabasic and basic composition.

PETROGRAPHIC AND GEOCHEMICAL CLASSIFICATION OF THE ROCKS

Petrographically, the Lukkulaisvaara rocks may be divided into three unequal units: 1) rocks with a cumulus texture, which form well-developed modal layering, 2) fine-grained rocks found as lenticular bodies with

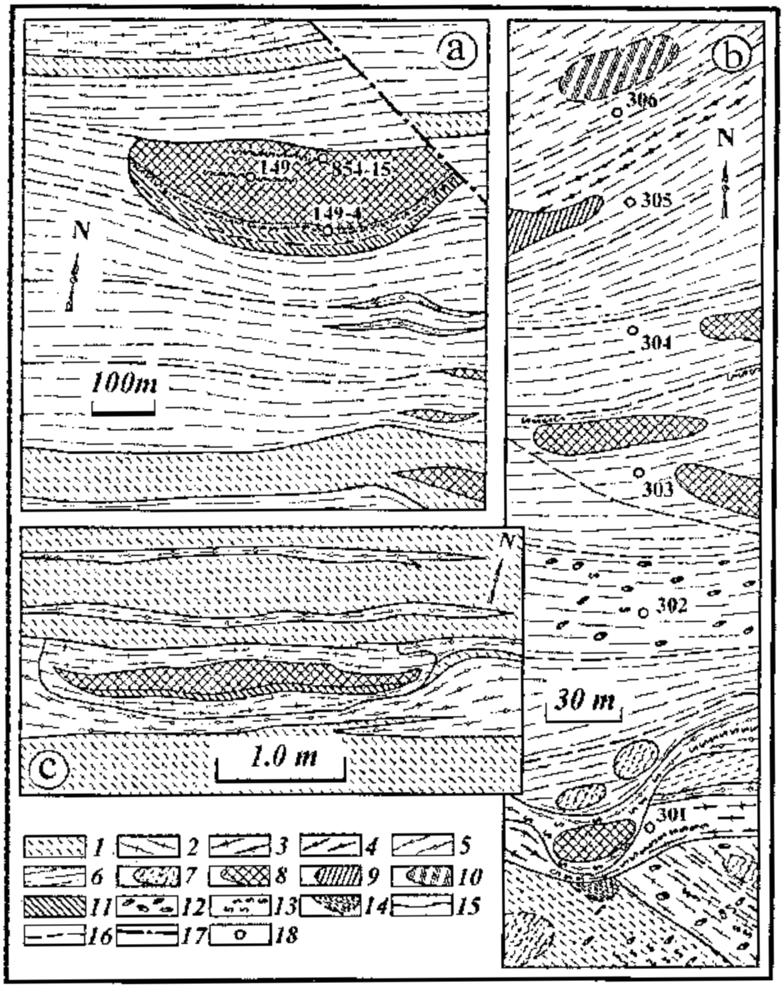

FIG. 3. Portions of outcrops with potholes. 1. Medium- to coarse-grained gabbronorite, 2. Coarse-grained gabbronorite, 3. Medium-grained norite, 4. Olivine-bearing gabbronorite, 5. Olivine-bearing melanocratic norite, 6. Coarse-grained norite, 7. Fine-grained rocks under the Quaternary deposits, 8. Fine-grained norite, 9. Fine-grained gabbronorite, 10. Geophysical anomaly, 11. Anorthosites, 12. Quartziferous gabbroic pegmatites, 13. Fe–Ni–Cu sulfide and PGE mineralization, 14. Thin layers, 15. Geological boundaries, 16. Geophysical boundaries, 17. Fault, 18. Sampling sites.

poorly developed or no modal layering, and 3) rocks of the vein facies. Within most of the rocks, two textural groups of minerals may be distinguished on the basis of their degree of idiomorphism. The first group includes euhedral and subhedral grains, with points, edges, or faces in contact to form a framework. The second group involves anhedral aggregates that fill the interstices between the euhedral crystals. Crystals of the first group are classified as of cumulus nature and are the result of crystal accumulation on the bottom of a chamber. Minerals of the second group are classified as being of intercumulus nature because they are the products of the subsequent crystallization of melt trapped between the cumulus minerals.

Petrography of rocks with a cumulus texture

Six types of cumulus assemblage are distinguished in rocks of the first group.

Olivine and olivine + chromian spinel cumulates are represented by olivinites and dunites. Olivine (Fo_{78-84}) may either show substantial adcumulus overgrowth, or may be resorbed and rimmed by postcumulus orthopyroxene ($En_{78–82}Wo_{3–4}Fs_{14–16}$). Fine-grained chromite is commonly disseminated in the dunite and concentrated in pyroxene or plagioclase. Postcumulus augite, augite–diopside ($En_{45–55}Wo_{31–46}Fs_{7–13}$) and plagioclase ($An_{67–70}$), in the form of subpoikilitic interstitial grains, are present in small quantities in virtually all the olivinites and dunites. Postcumulus biotite, where present, is a minor constituent.

Olivine + orthopyroxene ± chromian spinel cumulates are represented by harzburgites, with slightly varying proportions of the rock-forming minerals. Orthopyroxene ($En_{78–82}Wo_{3–5}Fs_{14–16}$) may occur as oikocrysts with embayed olivine ($Fo_{80–83}$) and chromite inclusions. Postcumulus diopside ($En_{49–53}Wo_{38–41}Fs_{8–10}$) and plagioclase ($An_{42–68}$) also occur.

Orthopyroxene cumulates are represented by orthopyroxenite. Olivine, where present, is a minor constituent. Orthopyroxene ($En_{80–82}Wo_{3–3.5}Fs_{14–17}$) may occur as oikocrysts with minor embayed inclusions of olivine. Postcumulus augite and plagioclase ($An_{67–69}$) are observed.

Orthopyroxene + plagioclase ± olivine cumulates are represented by norite and olivine-bearing norite, with varying relations of the rock-forming minerals and varying grain-size. In some rocks, poikilitic euhedral and subhedral grains of orthopyroxene with fine inclusions of plagioclase are present ($An_{53–78}$). The composition of the orthopyroxene is: $En_{68–80}Fs_{15–29}Wo_{1–4}$. The plagioclase in the matrix is usually patchily zoned ($An_{76–66}$). The grains of olivine ($Fo_{73–76}$) may be resorbed or rimmed by pyroxene. Postcumulus augite ($En_{41–48}Wo_{39–47}Fs_{9–14}$), in the form of poikilitic and subpoikilitic interstitial grains, also is present. Postcumulus interstitial grains of quartz and biotite may be present in coarse-grained norite.

Orthopyroxene + augite + plagioclase ± olivine cumulates are represented by gabbronorite and olivine-bearing gabbronorite, with varying relations of the rock-forming minerals and grain size. The composition of the pyroxenes is as follows: Opx: $En_{67–73}Wo_{3–5}Fs_{23–30}$; Cpx: $En_{43–48}Wo_{38–46}Fs_{10–15}$. Plagioclase is usually patchily zoned ($An_{60–70}$).

Plagioclase cumulates are represented by anorthosite and mottled anorthosite. Postcumulus pyroxenes are present in the form of subpoikilitic interstitial grains. Strong optical and chemical zoning is evident in plagioclase: rim $An_{55–60}$ and core $An_{65–70}$.

Lenticular bodies of fine-grained rocks

The fine-grained gabbronorite and norite are subdivided into two subtypes: rocks with grain sizes up to 0.5–0.6 mm, and distinctly trachytic rocks with grain sizes reaching 0.2 mm. In turn, fine-grained gabbronorite is subdivided into oikocrystic and equigranular types. The former occurs mainly in large bodies of fine-grained gabbronorite where they, together with oikocrystic and equigranular rocks, form a kind of autonomous differentiated series. Petrographic data distinguish six mineral assemblages in the fine-grained rocks: 1) {orthopyroxene} + clinopyroxene + plagioclase, 2) {orthopyroxene} + clinopyroxene + pigeonite + plagioclase, 3) clinopyroxene + pigeonite + plagioclase, 4) clinopyroxene + plagioclase, 5) orthopyroxene + plagioclase + [clinopyroxene], 6) orthopyroxene + [plagioclase + clinopyroxene]. Assemblages 2 and 3 occur only in the central part of large (up to 100 m thick) lenticular bodies of fine-grained gabbronorite. Rocks displaying assemblage 4 form small bodies and the central part of large bodies, whereas rocks with assemblage 1 form the rim of large bodies. Rocks with assemblages 5 and 6 form mainly separate bodies. Orthopyroxene ($En_{72.5–75.4}Wo_{19.8–24.2}Fs_{2.6–4.7}$) is present as large (up to 10 mm and over) oikocrysts in assemblages 1 and 2, with inclusions of plagioclase crystals even finer (up to 0.1 mm) than plagioclase in the matrix of the rock (the plagioclase in the matrix and in inclusions is $An_{67–70}$ and $An_{67–76}$, respectively), and, locally, clinopyroxene (clinopyroxene in the matrix and in inclusions is $En_{44.0–49.2}Wo_{38.6–44.4}Fs_{9.0–13.2}$). The proportion of oikocrysts may attain about 50 vol.%, whereas the content of plagioclase and clinopyroxene in the rock varies between 30–45% and 20–25%, respectively. The fine-grained matrix locally contains grains of pigeonite idiomorphically similar to augite (assemblages 2, 3). It should be noted that pigeonite inverted to orthopyroxene with a characteristic herringbone structure of solid-solution decomposition (matrix of inverted pigeonite $En_{72–75}Wo_{3–5}Fs_{22–24}$, inclusions $En_{44–49}Wo_{38–45}Fs_{9–13}$). Attention is drawn to the similar orientation of separate crystals of inverted pigeonite characterized by domains (up to 10 mm across). As a rule, the rocks of this group (in particular, fine-grained gabbronorite, which forms thin lenticular and vein-like bodies) are strongly altered.

Fine-grained norite (mineral assemblage 5) is similar to fine-grained gabbronorite in texture, but the clinopyroxene ($En_{45–46}Fs_{9–10}Wo_{44–45}$) fills the interstices between euhedral crystals of orthopyroxene ($En_{78–79}Fs_{19–20}Wo_{2–3}$) and plagioclase. In addition, clinopyroxene contains large poikilitic crystals (up to 8 mm across) containing microcrysts of orthopyroxene and plagioclase ($An_{78–82}$). Plagioclase in the rock matrix is usually patchily zoned ($An_{65–67}$). Poikilitic fine-grained norite in which idiomorphic crystals of ferroan enstatite are enriched in microcrystals of plagioclase are unique to these rocks.

Fine-grained poikilitic pyroxenites contain large poikilitic grains of clinopyroxene (up to 6 mm across) containing microcrysts of orthopyroxene. Orthopyroxene forms euhedral crystals commonly with very small inclusions of plagioclase. Disseminated fine-grained chromite (up to 0.2 mm) was found in several samples.

Rocks of the vein facies

Rocks without cumulus textures are relatively rare. They occur as vein-facies lithologies (ore-bearing pegmatitic gabbronorite, pyroxenite, their barren equivalents, and quartziferous gabbroic pegmatites). In ore-bearing gabbronorite, orthopyroxene ($En_{72–74}Fs_{22–24}Wo_{4–5}$) and clinopyroxene ($En_{47}Fs_{42–43}Wo_{10–11}$) display a more idiomorphic habit than plagioclase ($An_{67–70}$). Interstices are filled with aggregates of Cu–Fe–Ni-sulfides, reaching 30 vol.%. Rocks of this group are strongly altered. Barren gabbronorite and pyroxenite of the vein facies do not differ texturally from their ore-bearing equivalents, but they show no evidence of deuteric alteration.

Quartziferous gabbroic pegmatite forms individual segregations, about 1 m across, and veins a few tens of centimeters thick. Bluish quartz (up to 5%) is characteristic of the rocks. They are strongly altered with unidentifiable mafic minerals and disseminated sulfide aggregates.

Hydrothermal alteration

Unaltered or weakly altered rocks make up about 30% of the layered series, but a high degree of hydrothermal alteration is typical of sulfide-bearing rocks with Pt-mineralization. Veins range from very narrow (<1 mm) to several centimeters in width, commonly with many branches. Mineral assemblages in the veins are varied: 1) hornblende (varying compositions), 2) hornblende and scapolite with minor biotite and plagioclase, 3) hornblende with disseminated sulfides, 4) carbonates (calcite and dolomite) with scapolite, 5) quartz, chlorite and calcite. These assemblages may change significantly along strike, but the contacts of the veins with the host rocks are, as a rule, sharp. The fresh rocks of the intrusion are characterized by the presence of zones of recrystallization, in some cases with a zonal structure, for instance scapolite in the central part and zoisite with some chlorite grains at their margin.

The major secondary mineral assemblages may be divided into two groups: 1) M1: a) talc + anthophyllite + actinolite + sulfides + magnetite, b) talc + anthophyllite + actinolite + hornblende (blue-green) + chlorite + plagioclase + sulfides + magnetite; M2: a) actinolite + hornblende (green, pale green, blue-green) + clinozoisite ± epidote + chlorite + plagioclase ± muscovite, b) actinolite + hornblende (green, pale green, blue-green) + clinozoisite ± epidote + chlorite + plagioclase + biotite (secondary), c) actinolite + hornblende (green, pale green, blue-green) + clinozoisite ± epidote + chlorite + biotite (secondary) + scapolite + plagioclase ± carbonates, d) actinolite + hornblende (pale green) + clinozoisite ± epidote + chlorite + garnet + plagioclase.

The M1 assemblages are typical of the veins of altered ore-bearing bronzitites (M1a) and gabbronorites (M1b). The M2 assemblages are typical of altered norites, gabbronorites and anorthosites of the layered series. M2 may also involve staurolite (Barkov *et al.* 1999), quartz, albite and anorthite (M2abc), K-feldspar together with sulfides (M2a), prehnite, pumpellyite and segregations of zeolite (M2ab). Talc and anthophyllite may be present as relics. These assemblages are divided into Fe–Ni–Cu sulfide-bearing, PGM-bearing and ore-free assemblages.

Recrystallization of the primary mineral assemblages resulted in the development of reaction rims replacing the igneous minerals. Different types of reaction structures can be distinguished in the rocks. For example, the reaction rim developed between two adjacent grains of orthopyroxene are symmetrically zoned and consist of outer talc + anthophyllite shells (next to orthopyroxene) and inner hornblende shells. At contacts with igneous plagioclase, orthopyroxene is replaced by (from orthopyroxene to plagioclase) talc + anthophyllite or talc + anthophyllite ± hornblende shells. Clinozoisite and albite commonly replace the marginal parts of plagioclase grains. Garnet and amphibole reaction rims were observed around relict orthopyroxene and along the cracks in plagioclase in gabbronorite. Very fine-grained garnet (less than 0.01 mm) in some cases forms equigranular aggregates up to 0.2 mm across, or skeletal crystals enclosing small plagioclase grains. Also, garnet comprises the axial parts of hornblende–garnet segregations in fine-grained gabbronorite. Garnet was discovered in the assemblages with sulfides. In the totally recrystallized lithologies, aggregates of secondary minerals completely replace the primary igneous minerals.

High contents of chlorine were determined in secondary biotite (up to 0.55 wt%), Al-rich amphiboles (up to 2.5 wt%), chlorite (up to 0.1 wt%), and scapolite (up to 2.3 wt%) from ore-bearing mineral assemblages.

Fe–Ni–Cu SULFIDE AND PGM MINERALIZATION

Sulfides

Two main genetic types of sulfide were encountered: a) sulfides of the magmatic stage are present in unaltered rocks of the layered series and in bronzitite and gabbronorite of vein-facies rocks within the bodies of fine-grained gabbronorite, b) sulfides of the metamorphic stage occur along the internal angular unconformity of potholes and near the contact of large bodies of fine-grained rock types with the underlying layers of potholes and along the cracks formed during late stages of deformation. Sulfides of type (a) occur locally in association with magnetite, quartz and biotite of the magmatic stage, as inclusions in magmatic minerals (usually pyroxene), and in the vein-facies rocks, where sulfides and magnetite with M1 mineral assemblages fill the space between orthomagmatic minerals (their presence suggests a melt) or form microveins that cut both plagioclase and ferroan enstatite. Sulfides of type (b) occur as fine disseminations and clusters, and form segregations with secondary mineral assemblages (M2) such as zoisite + amphiboles + chlorite, scapolite + carbonate minerals, quartz + amphiboles + zoisite + chlorite, and amphiboles + garnet. The amount of sulfides varies up to 30 vol.% in type (a) and 5–10 vol.% in type (b).

Sulfides of the M2 assemblage occur near the contact of the large bodies of fine-grained lithologies with the underlying layers of the stratified series (rocks of the footwall units, *i.e.*, anorthosite, gabbronorite and the melanocratic olivine-bearing norite). The ore-bearing (M2) assemblage is also typical of the gabbronorite occurring along the internal angular unconformity, manifesting itself as a drastic change in layering and trachytic texture (Fig. 3). Veins and segregations of quartziferous pegmatitic gabbro impregnate them.

Sulfides of the M1 assemblage are subdivided into three varieties (Table 1). Assemblages 1 and 2 are predominant. Usually, pentlandite forms inclusions in chalcopyrite and is replaced by violarite and pyrite. Fine grains of marcasite replace pyrrhotite. The size of the sulfide minerals in this type of rock reaches several millimeters, with sulfide aggregates controlled by the geometry of interstitial space between the igneous minerals, giving a "sideronitic" texture. The borders of the ore minerals are very irregular and, together with secondary minerals, penetrate into the crystals of ferroan enstatite or plagioclase. Fine grains of sulfides usually occur in microveins and in pseudomorphs of actinolite, talc and anthophyllite at the expense of pyroxenes. The replacement of pyroxenes by sulfide grains is observed in rocks comprising up to 40 vol.% of ore minerals. Sulfides of the M2 assemblage are represented by one type (Table 1), whose proportions can be correlated with the degree of recrystallization of the rocks. Inclusions of chlorite, titanite, amphiboles, zoisite, scapolite, rare K-feldspar, and albite are typical for sulfides. Aggregates of sulfides and garnet were found.

TABLE 1. SULFIDE ASSEMBLAGES, LUKKULAISVAARA LAYERED INTRUSION, NORTHERN KARELIA

	Mineral assemblages					Mineral assemblages			
	1	2	3	4		1	2	3	4
Pyrrhotite	M	M	-	-	Marcasite	R	R	-	-
Pentlandite	M	M	M	M	Sphalerite	R	R	R	R
Chalcopyrite	M	M	M	M	Bornite	-	-	R	Mi
Cubanite	-	R	-	-	Chalcocite	-	-	-	R
Millerite	-	-	R	Mi	Galena	R	R	-	-
Violarite	Mi	Mi	Mi	R	Greenockite	-	-	-	R
Polydymite	-	-	R	R	Heazlewoodite	-	-	-	R
Pyrite	Mi	R	-	-	Godlevskite	-	-	-	R

1–4: mineral assemblages. 1: sulfides from rocks at the exocontacts of the large bodies of fine-grained gabbronorite. 2, 3, 4: sulfides from the veins of pyroxenite and gabbronorite within the bodies of fine-grained gabbronorite. The associations: 2: chalcopyrite – pyrrhotite – pentlandite, 3: chalcopyrite – pentlandite, 4: pentlandite – violarite – millerite – bornite – chalcopyrite with magnetite. M: main mineral, Mi: minor mineral, R: rare mineral.

Platinum-group minerals

The PGM are observed in practically all sulfide-bearing platinum-group-element (*PGE*) horizons (Table 2). The richest mineralization is related to the altered bronzitite and gabbronorite veins enriched in sulfides (M1), and the strongly altered anorthosite, gabbronorite and norite with poor sulfide mineralization near contacts with large bodies of the fine-grained lithologies (M2). The total concentration of Pd and Pt is in the range 0.3–10 ppm Pt and 0.42–66 ppm Pd (Table 3). Among

TABLE 2. MINERALS OF THE NOBLE METALS, LUKKULAISVAARA LAYERED INTRUSION

	Minerals	Formulas	1	2	3	4
1	Kotulskite	Pd(Te,Bi,Pb)	M	M	M	M
2	Stibian kotulskite	$Pd_{1-x}(Te,Sb)$	R	R	R	-
3	Merenskyite	$Pd(Te,Bi)_2$	M	M	M	R
4	Nickeloan merenskyite	$(Pd,Ni)Te_2$	-	R	R	R
5	Moncheite	$(Pt,Pd)(Te,Bi)_2$	M	M	R	M
6	Hessite	Ag_2Te	-	R	M	-
7	Palladian and platinian melonite	$(Ni,Pd,Pt)Te_2$	R	-	R	R
8	Telluropalladinite	Pd_9Te_4	-	-	-	R
9	Sopcheite	$Ag_4Pd_3Te_4$	-	-	Mi	R
10	Telargpalite	$(Pd,Ag)_3(Te,Bi)$	-	-	R	Mi
11	Michenerite	PdBiTe	-	-	Mi	-
12	Sobolevskite	Pd(Bi,Te)	-	-	R	-
13	Froodite	$Pd(Bi,Te)_2$	-	-	R	-
14	Sperrylite	$PtAs_2$	M	M	M	R
15	Majakite	PdNiAs	Mi	R	R	-
16	Palladoarsenide	$(Pd,Ni)_2As$	R	-	R	-
17	Stillwaterite	$(Pd,Au)_8As_3$	R	-	-	-
18	Vysotskite	(Pd,Pt,Ni)S	R	-	-	-
19	Argentopentlandite	$Ag(Fe,Ni)_8S_8$	-	R	-	-
20	Hollingworthite	(Rh,Pt,Ir,Os,Ru, Fe,Ni,Co)AsS	R	R	R	-
21	Irarsite	(Ir,Rh,Pt,Pd,Fe)AsS	R	R	-	-
22	Isomertieite	$Pd_{11}Sb_2As_2$	-	-	R	-
23	Mertieite I	$Pd_{11}(Sb,As)_4$	-	-	R	-
24	Mertieite II	$Pd_8(Sb,Sn,As)_3$	R	-	R	-
25	Tulameenite	Pt_2FeCu	-	-	R	Mi
26	Hongshiite	PtCu	-	-	-	R
27	Gold	(Au,Ag)	R	R	-	-
28	"Electrum"[1]	(Au,Ag)	-	-	R	R
29	"Küstelite"[1]	Ag_3Au	-	-	R	R
30	Zvyagintsevite	$Pd_3(Pb,Bi)$	-	-	R	Mi
31	Paolovite	Pd_2Sn	-	R	R	-
32	Taimyrite*	$(Pd,Cu,Pt)_3Sn$				
33	Oulankaite	$(Pd,Pt)_5(Cu,Fe)_4SnTe_2S_2$	-	-	-	R
34	Unnamed	Pd_2TeBi	-	-	Mi	-
35	Unnamed	$Pd_2(Te,Pd,Bi)$	-	-	R	R
36	Unnamed	$(Pd,Ag)_2Te$	-	-	-	R
37	Unnamed	$Pd_{21}Ag_4Te_7$	-	-	-	R
38	Unnamed	$Pd_2(Sb,Sn)$	-	-	R	m
39	Unnamed*	$PtAs_2S_4$				
40	Unnamed*	$Pd_2(Cu,Ag)_2S_3$				
41	Unnamed*	Pd_8Te_3				
42	Unnamed*	Pd_6AgTe_4				

Columns: 1 Mineral assemblages at the exocontacts of the large bodies of fine-grained rocks (sulfide association: pyrrhotite – pentlandite – chalcopyrite). 2–4 Veins of pyroxenites and gabbronorites within bodies of fine-grained gabbronorite are enriched in sulfides. The associations: 2: chalcopyrite – pyrrhotite – pentlandite, 3 chalcopyrite – pentlandite, 4: pentlandite – violarite – millerite – bornite chalcopyrite with magnetite. M: main mineral, Mi: minor mineral, R: rare mineral.

* Minerals determined by T.L. Grokhovskaya (Klyunin *et al.* 1994).

[1] Quotation marks are used to show that these are not IMA-approved names; Simusikov & Pavlova (2000) have shown that "küstelite" is a mixture of pure gold and pure silver of bulk composition Ag_3Au.

TABLE 3. CHEMICAL COMPOSITION OF ORE-BEARING ROCKS, LUKKULAISVAARA INTRUSION, NORTHERN KARELIA

	1	2	3	4	5	6	7	8	9	10	11	12
SiO_2 wt%	46.00	41.22	46.32	31.80	31.80	49.66	44.64	44.80	49.98	42.44	44.66	48.56
TiO_2	1.00	0.13	0.16	0.07	0.09	0.13	0.56	0.28	0.18	0.19	0.13	0.16
Al_2O_3	13.70	13.23	13.73	2.85	2.78	13.96	21.68	20.32	26.00	26.10	25.27	14.24
Fe_2O_3	3.73	8.56	3.94	14.00	10.87	1.00	1.15	1.50	0.14	1.94	1.11	0.46
FeO	6.32	5.17	6.32	6.32	4.90	6.32	4.60	5.17	2.87	3.74	4.02	5.75
MnO	0.32	0.19	0.27	0.27	0.27	0.27	0.22	0.28	0.22	0.24	0.16	0.28
MgO	10.85	9.85	11.55	11.26	12.46	10.65	6.03	7.54	2.11	1.91	2.41	11.86
CaO	9.80	10.21	10.63	8.11	9.23	13.14	13.00	12.30	7.97	16.78	10.70	13.70
Na_2O	1.59	0.98	1.52	0.11	0.10	1.75	2.02	1.68	5.19	2.15	3.16	1.75
K_2O	0.13	0.10	0.19	0.05	0.03	0.17	0.39	0.28	1.92	0.15	0.25	0.16
P_2O_5	0.04	0.04	0.05	0.07	0.06	0.06	0.18	0.04	0.03	0.02	0.02	0.04
H_2O 105°C	0.06	0.04	0.08	0.66	0.30	0.30	0.14	0.20	0.14	0.12	0.16	0.30
L.O.I.	2.30	3.91	2.50	7.90	1.94	0.70	3.31	2.31	3.01	1.86	2.71	1.94
Ag ppm	9.30	6.93	5.96	6.51	13.90	0.92	0.14	0.13	0.018	0.12	0.13	0.68
Au	0.16	0.16	0.16	0.26	1.17	0.08	0.39	0.29	0.02	0.42	0.33	0.03
Pt	3.90	6.90	5.50	1.23	1.45	0.30	2.47	2.08	1.10	1.04	1.22	0.11
Pd	13.00	24.00	18.50	66.40	24.00	0.95	6.02	5.14	4.40	4.79	5.34	0.42
Ru ppb	1.30	17.80	0.20	32.90	12.10	0.91	2.90	1.41	0.70	1.26	2.19	0.15
Rh	0.15	1.73	0.20	5.55	2.10	0.20	0.20	0.22	0.20	0.30	0.20	0.20
Zn ppm	150	240	200	100	600	160	160	150	100	150	100	100
Cu	35000	46800	40200	120300	120300	2180	4344	3160	674	4670	2950	1704
Pb	10	10	10	10	10	10	10	10	10	10	10	10
Co	73	411	78	340	361	750	85	80	35	92	78	77
Ni	2334	18100	2327	20000	17200	1000	2300	800	173	1917	1822	1192
Cr	241	205	268	190	249	333	75	100	65	75	75	100

Columns 1–5: Veins of altered ore-bearing pyroxenite from the body of the fine-grained gabbronorite. Ath + Act + Tlc at the expense of Opx: 70–75 vol.%, ore minerals (bornite + millerite + pentlandite + magnetite + chalcopyrite): 25–30 vol.% (samples Lu 149, Lu 149a, Lu 149b), ore minerals (pentlandite + violarite + chalcopyrite): 25 vol.% (samples Lu 80b, Lu 80z). 6: Veins of ore-bearing norite from the body of fine-grained gabbronorite. Pl (An_{65-68}): 40%, Opx: 50%, ore minerals (pentlandite + pyrite + violarite + pyrrhotite+chalcopyrite):10%, Hbl + Czo with minor garnet at the expense of plagioclase (Lu–Ka–20–56). 7: Altered ore-bearing anorthosite. Relics of Pl: 45 vol.%, Ep + Czo at the expense of Pl: 25 vol.%, relics of Cpx: 5 vol.%, Act at the expense of Cpx: 10 vol%, ore-minerals (pentlandite + pyrite + violarite + chalcopyrite): 10 vol.%, Qtz: 3 vol.%, prehnite: 2 vol.% (sample Lu 828). 8, 9: Altered anorthosite. Relics of Pl (An_{65-67}): 75 vol.%, Ep + Czo at the expense of Pl: 5–10 vol.%, ore minerals (see sample 6): 10 vol.%, Chl: 5 vol.% (samples Lu 830, Lu 832). 10: Altered anorthosite. Czo+Ep: 75 vol.%, ore minerals (see sample 6): 10 vol.%, Chl: 10 vol.%, Qtz: 5 vol.% (sample Lu 837). 11: Altered anorthosite. Relics of Pl (An_{25-40}): 45 vol.%, relics of Cpx: 1–3 vol.%, prehnite: 20–25 vol.%, Ep+Czo: 25 vol.%, ore minerals (see sample 6): 3–5 vol.%, Qtz: 1–2 vol.% (sample Lu 838). 12: Altered fine-grained gabbro-norite with disseminated sulfides. The rock is crossed by prehnite veins. Mineral composition: fine-grained gabbro-norite: Pl: 45 vol.%, Opx: 10–15 vol.%, Cpx: 30 vol.%; prehnite veins: prehnite 95–97 vol.%, sulfides: 3–5 vol.% (sample Lu 815).

the PGM are tellurides, and solid-solution series minerals between PGE tellurides and PGE bismuthides, and sulfarsenides. Other mineral groups (sulfides, antimonides, and alloys) are of minor importance. Combinations of Te, Bi, As with Pd, Pt and Ag make up almost half of all established types of minerals of the noble elements. They are subdivided in two groups: 1) bismuth tellurides and bismuthides of Pd and Ag, and 2) tellurides of Pd and Ag. Combinations of Pd with As and Sb are also common among these minerals. The widest spectrum and largest grains of platinum-group minerals occur with rich sulfide ores in the altered bronzitite and gabbronorite of the vein facies. PGM are mostly (95%) associated with chalcopyrite, but intergrowths of PGM with pyrrhotite, pentlandite, pyrite, violarite, millerite and bornite also occur. The PGM are related to a relatively late stage of mineral formation, and they fill the interstices between grains of secondary minerals and between sulfide grains. The crystallization of the earliest kotulskite and merenskyite together with secondary quartz and calcite testify that crystallization of PGM took place under the same conditions as those that formed the secondary minerals.

GEOCHEMICAL CLASSIFICATION OF THE ROCKS

For this study, 128 samples representing rocks of the layered series and 68 samples of the fine-grained lithologies were selected. These samples characterize more or less all the common rocks of the intrusion. Cluster analysis was used to determine: a) the petrochemical types of rocks, as hydrothermal alteration made petrographic characterization difficult, and b) the relations between identified geochemical groups of rocks (fine-grained and coarse-grained), in order to evaluate our suggestion concerning a link between the fine-grained rocks and an additional episode of emplacement.

TABLE 4. CHEMICAL COMPOSITION OF THE PETROCHEMICAL TYPES (CLUSTERS) OF ROCK FROM THE LAYERED SERIES, WITH NORMS, LUKKULAISVAARA INTRUSION

Cumulates	Ol = Opx			Opx + Pl ± Ol						Opx – Cpx + Pl ± Ol					Pl
	1	2	3	4	5	6	7	8	9	10	11	12	13	14	15
SiO_2 wt%	43.78	43.92	44.90	51.43	52.64	53.60	52.32	50.14	51.64	53.14	52.19	51.27	52.55	52.45	51.65
TiO_2	0.24	0.34	0.27	0.24	0.24	0.31	0.24	0.25	0.34	0.35	0.26	0.36	0.30	0.24	0.24
Al_2O_3	4.44	3.57	5.79	8.32	14.07	15.46	18.31	18.73	22.59	8.20	13.92	10.92	16.38	15.97	26.57
FeO	12.92	13.70	12.29	10.12	7.05	7.69	6.36	6.81	4.78	8.87	6.65	10.59	7.85	6.16	2.47
MnO	0.19	0.21	0.18	0.22	0.16	0.18	0.13	0.13	0.10	0.19	0.17	0.17	0.17	0.15	0.06
MgO	34.36	34.91	31.53	23.25	15.46	11.47	10.34	11.18	6.16	18.93	12.39	15.34	9.05	10.74	3.10
CaO	3.31	3.00	4.49	5.67	9.00	9.08	9.91	10.69	11.67	9.70	12.05	9.80	11.23	12.39	11.71
Na_2O	0.55	0.17	0.43	0.53	1.16	1.86	1.98	1.76	2.29	0.51	1.34	1.16	2.11	1.66	3.25
K_2O	0.20	0.16	0.19	0.18	0.17	0.34	0.37	0.27	0.41	0.07	0.21	0.36	0.33	0.22	0.88
P_2O_5	0.01	0.04	0.03	0.04	0.05	0.02	0.04	0.05	0.06	0.05	0.04	0.05	0.01	0.03	0.06
Pl vol.%	18.1	13.3	21.6	29.5	48.5	55.9	64.0	64.1	76.2	28.2	48.5	40.5	59.3	55.5	90.4
Cpx	6.2	5.8	7.5	6.8	9.4	9.4	7.0	8.1	5.6	22.8	25.1	20.0	16.5	19.8	2.0
Opx	8.7	16.2	14.7	49.8	51.1	33.0	27.5	18.8	17.4	47.8	24.2	29.8	23.1	24.2	3.8
Ol	66.7	64.3	55.8	13.6	0.8	0.0	1.2	8.7	0.0	0.7	2.0	9.2	0.8	0.1	3.5
Ilm	0.3	0.4	0.3	0.3	0.3	0.4	0.3	0.3	0.4	0.4	0.3	0.4	0.4	0.3	0.3
Qtz	0.0	0.0	0.0	0.0	0.0	1.3	0.0	0.0	0.5	0.0	0.0	0.0	0.0	0.0	0.0
f*	0.18	0.18	0.18	0.20	0.21	0.28	0.26	0.26	0.31	0.21	0.24	0.28	0.33	0.25	0.31
An**	0.60	0.78	0.73	0.77	0.74	0.64	0.67	0.71	0.69	0.80	0.70	0.65	0.62	0.69	0.62

* f = Fe/(Fe + Mg); ** An: plagioclase composition.

As a result of the cluster analysis, 15 petrochemical types (clusters) were defined for rocks of the layered series and named after their normative composition (Table 4). These chemical types form four groups characterized by different cumulate assemblages. The first cluster represents the olivinites, dunites and harzburgites (olivine and olivine + orthopyroxene as cumulus mineral assemblages). The next eight clusters include one of the most abundant rock-types and are represented by norite and olivine-bearing norite (the plagioclase – orthopyroxene ± olivine cumulus mineral assemblages). Gabbronorite (plagioclase – orthopyroxene – clynopyroxene ± olivine cumulus mineral assemblage), the most abundant rock type, forms five clusters. The last cluster is represented by anorthosite (plagioclase cumulus assemblages). The chemical and textural types of the rocks are well correlated. On the basis of these data, we consider combining the separate parts of the sections 2–2 and 3–3. The boundary is located between leucocratic norite and gabbronorite (the samples from the overlapping parts of different sections fall into the same cluster,10, and the samples numbered Lu 304, Lu 622, 623 can be taken as marker beds (Fig. 4).

The chemical and normative compositions of the fine-grained rocks are given in Table 5. Six clusters were defined for the fine-grained rocks (Table 6); the first three are represented by gabbronorite, and the others by norite. Comparison of chemical types of the fine-grained and layer-forming rocks shows that there are no differences in terms of the chemical and normative compositions of the clusters (Fig. 5), their Fe number (f), and the composition of the plagioclase (Tables 4, 6).

VERTICAL SEQUENCE OF THE INTRUSION

The vertical sequence can only be represented by constructing a composite section owing to the asymmetrical structure of the intrusion and the poor exposure of some portions of the layered series (Fig. 2). As noted above, when compiling the whole section of the Lukkulaisvaara massif from the 2–2 and 3–3 sections, the boundary between leucocratic norite and gabbronorite, traced throughout the axial zone of the massif, was taken as a marker. Parts of the whole profile (Fig. 2) were joined using petrographic, petrochemical, and geochemical data, as well as the results of the cluster analysis. The layered series was divided into zones characterized by a specific assemblage of cumulus minerals. This enabled us to establish the order in which solid phases filled the intrusive chamber and to clarify the regularities of the initial crystallization of the magma.

The layered series of the intrusion is represented by the following zones (from south to north): ultrabasic zone, norite-I zone, gabbronorite-I zone, norite-2 zone, gabbronorite-2 zone (Figs. 4, 6c). From south to north, the number of phases in the cumulative parageneses increases, and high-temperature parageneses give way to low-temperature parageneses. It is known that the chambers of layered intrusions are filled by solid phases from the bottom upward. Therefore, the present southern contact of the massif was originally the bottom, and the northern contact was the roof of the intrusion. On the basis of these data, the vertical sequence, if viewed from the point of the distribution of cumulative rocks only, can be presented as follows: 1) Lower marginal zone, up to 150 m thick. 2) Zone of interlaminated dunite, olvinite, harzburgite, and olivine bronzitite (DHZ), up to 450 m. 3) Norite-I zone (NZ–I), made up of norite with rare layers of gabbronorite, more than 900 m. 4) Gabbronorite-I zone (GNZ–I), made up of gabbronorite with lenticular bodies of fine-grained gabbronorite, rare layers of norite and olivine-bearing rocks (troctolite, olivine gabbronorite), up to 700 m. 5) Norite-2 zone (NZ–2), made up of mesocratic to leucocratic norite, containing separate lenses of fine-grained gabbronorite, norite (quite variable in thickness) overlying olivine-bearing rocks (commonly olivine-bearing gabbronorite). NZ–2 varies in thickness, with an average of 160 m. 6) Gabbronorite-2 zone (GNZ–2) made up of gabbronorite, containing separate layers of norite, up to 1670 m. 7) Upper marginal zone (UMZ), made up of gabbronorite, up to 620 m.

The Lukkulaisvaara intrusion contains two subzones with structures comparable to the potholes of the Bushveld Complex. The first, thickest and most prominent subzone is where part of the gabbronorite-I zone rests upon mesocratic norite (norite-I zone). The second subzone occurs at about 200 m above the gabbronorite-I zone, where it disconformably overlies a thick layer of leucocratic norites of the norite-II zone. Figure 3 demonstrates typical outcrops of the potholes. Potholes are extremely variable in size from a few tens of centimeters to a few tens and even hundreds of meters in thickness and strike (Fig. 3). The bottom and top of the potholes are usually conformable to the layering of the intrusion, whereas their flanks transect the layering. Marker horizons underlying the bottom of the potholes commonly are intensely mineralized with stratiform and

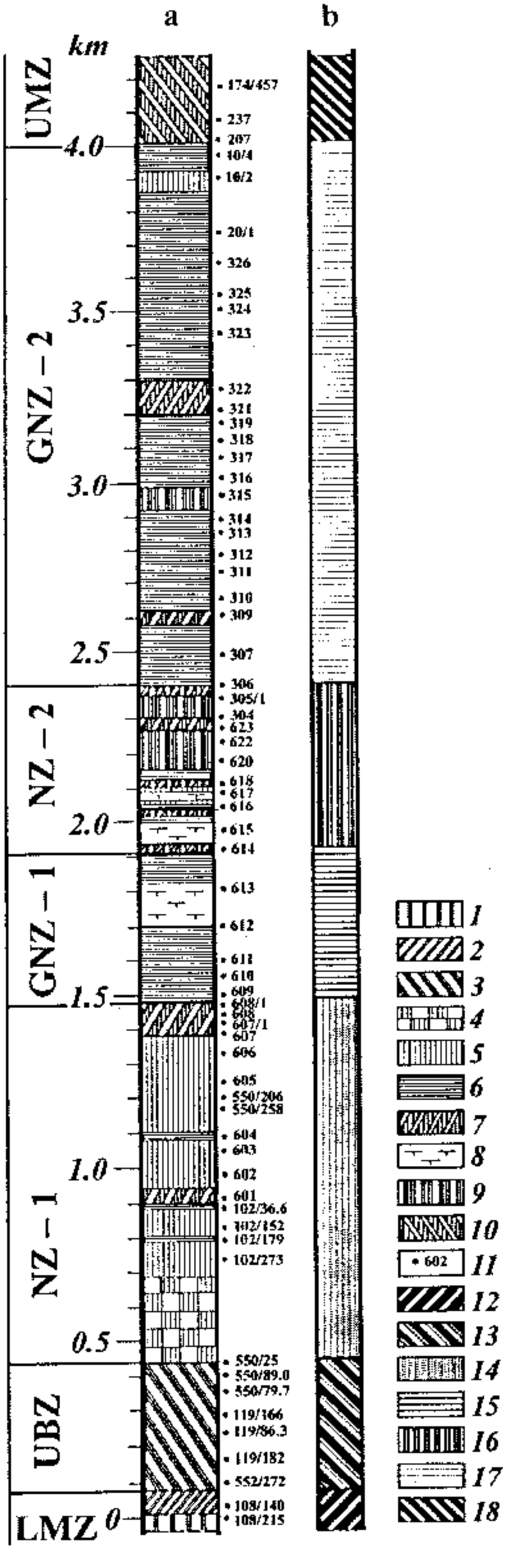

FIG. 4. a. Distribution of the rock types (clusters) within the Lukkulaisvaara vertical section. b. Generalized scheme of distribution of the petrochemical types of rocks (clusters). Column a, 1. Cluster 14: gabbronorite of lower marginal zone, 2. Cluster 3: melanocratic olivine-bearing norite of lower marginal zone, 3. Cluster 1: olivinite and harzburgite of ultrabasic zone, 4. No data about the section, 5. Clusters 5, 9: norite of norite-1 zone, 6. Clusters 10, 11, 12, 13: gabbronorite of gabbronorite-1 and -2 zones, 7. Cluster 6: olivine-bearing norite of norite-1, -2 and gabbronorite-2 zones, 8. Cluster 4: fine-grained rocks, 9. Clusters 8, 15: leuconorite and anorthosite of norite-2 zone, 10. Clusters 2, 7: norite of upper marginal zone, 11. Sampling sites. Column b 12. Lower marginal zone (LMZ), 13. Ultrabasic zone (UBZ), 14. Norite-1 zone (NZ-1), 15. Gabbronorite-1 zone (GNZ-1), 16. Norite-2 zone (NZ–2), 17. Gabbronorite-2 zone (GNZ–2), 18. Upper marginal zone (UMZ).

TABLE 5. CHEMICAL COMPOSITION OF FINE-GRAINED ROCKS, WITH NORMS, LUKKULAISVAARA INTRUSION

H, m	Sample	SiO_2	TiO_2	Al_2O_3	FeO *	MnO	MgO	CaO	Na_2O	K_2O	P_2O_5	Fe_2O_3	Pl	Cpx	Opx	Ol	Ilm	Qtz	f **	An ***
First body of the fine-grained rocks																				
0.3	1-505	50,45	0,18	15.68	5.05	0.13	11,67	13.02	0.78	0.09	0.03	5.61	51.7	20.2	26.0	0.0	0.2	1.8	0.20	0,84
2.4	1-507	50,53	0.19	16.04	5.19	0.13	11.17	12.70	1.15	0.13	0.02	5.77	54.5	19.5	25.2	0.0	0.2	0.6	0,21	0,78
9.1	1-508	49.85	0.18	16,39	5,70	0.14	10.74	13.00	1.06	0.13	0,03	6,34	55.3	19.7	24.8	0.1	0.2	0.0	0.23	0.79
20.1	1-510	50.97	0.19	16.51	5.24	0,13	10.46	12,76	1.03	0.10	0.03	5.82	55.0	18.2	24.0	0.0	0.2	2.6	0,22	0,80
27.1	1-511	51.38	0.22	15.99	5.53	0.13	10.98	12.83	0,96	0,12	0.04	6,15	52.9	19.3	25.0	0.0	0.3	2.5	0.22	0.81
36.8	1-513	50.15	0,16	16.17	5.34	0.14	10,76	12,90	1.04	0.09	0.02	5.93	54.5	19.6	24.6	0.0	0.2	1.1	0.22	0.80
43.8	1-514	50,83	0,16	16.55	5.27	0.14	10.45	12,87	1,12	0.13	0.03	5.86	55.6	18.9	23.7	0.0	0.2	1.6	0.23	0,79
47.7	1-515	50.73	0.16	16,75	5.08	0.14	11.12	12.97	1.17	0,07	0,02	5.65	55,9	18,7	24.9	0.0	0.2	0.3	0.21	0.79
52.0	1-516	50,90	0.14	16.42	5.15	0,13	10,91	13.09	1.44	0.05	0.03	5.72	56.0	20.8	21.9	1,1	0,2	0.0	0.21	0.74
56.3	1-517	51.00	0,15	16.25	5.08	0.14	10.82	13.49	0,95	0.05	0.03	5.65	53.4	21.1	23.3	0.0	0.2	2.0	0.21	0,82
63.8	1-519	50.94	0.15	16.40	5 07	0.14	11.28	12.92	1.02	0.05	0.02	5.64	54,2	18.8	25,4	0.0	0.2	1.4	0.21	0.81
72.3	1-521	50.89	0.16	16,75	4.98	0.14	11.11	13.21	0.98	0.05	0,02	5.54	54.8	18.9	24.6	0.0	0.2	1.4	0.21	0.82
73.2	1-522	50.69	0.15	16.23	5.18	0.15	11.31	13.03	0.85	0.11	0,02	5,76	53.3	19.2	25.6	0.0	0.2	1.7	0.21	0.83
77.5	1-523	50.64	0.14	16.77	4.71	0.13	11.31	13.25	1.00	0.05	0.03	5.23	55.1	19.2	24.7	0.0	0.2	0,8	0,19	0.82
84.2	1-524	50.13	0.15	15,97	5.26	0.14	11.24	13.62	0,95	0,05	0.03	5.85	53.0	22.3	24.3	0.0	0.2	0.2	0,21	0.82
87.0	1-527	50,38	0,15	16.45	4.86	0.13	11,36	13,42	0.82	0.07	0.02	5.40	53.7	20,0	24,8	0,0	0,2	1.3	0.20	0.84
Second body of the fine-grained rocks																				
0,0	2006	51,20	0.06	18.10	5.83	0.12	9.00	12.70	1,90	0,07	0,03	6,48	62,4	17,1	18 6	1,9	0.1	0.0	0,27	0.70
9,4	2008	50.90	0.07	16.80	5,70	0.12	10,30	12,50	1.70	0,15	0.03	6,33	58,6	18,8	19.7	2.8	0.1	0.0	0.24	0.70
16	Lu 615	50.05	0.15	14.05	5.88	0,17	11.42	13,72	1.45	0.21	0.03	6.54	50.5	29.1	14.3	5.9	0.2	0.0	0.23	0.69
26	Lu2012	49.70	0.09	14.00	5.85	0.13	12.40	14.50	1.20	0.33	0.03	6.50	49.1	31.4	9.7	9.8	0.1	0.0	0.21	0.71
38	Lu2016	50.20	0.15	13.70	7.90	0.15	9.80	12.50	2.00	0.15	0.03	8.78	52.4	27.2	14.1	6.1	0.2	0.0	0.32	0.60
52	Lu2019	50.80	0.14	11.30	9.59	0.18	17.50	9.00	0.83	0.05	0.03	10.66	39.2	14.3	37.5	8.9	0.2	0,0	0.24	0,78
60	Lu2021	50.50	0.03	20.50	5.50	0.11	7.90	12.90	2.10	0.06	0,03	6 11	69.2	13,3	12,7	4,8	0,0	0,0	0,28	0.71
72	1016	50,40	0.10	13.27	6.02	0.12	12,72	12,78	1,68	0,09	0.05	6.69	48.9	27.7	15.2	8.1	0.1	0.0	0.21	0.65
73	Lu2025	50.40	0.03	19.20	5 14	0,10	10.30	12.30	1.60	0.08	0.03	5.71	64.0	12.2	19.7	4.0	0.0	0.0	0.22	0.75
77	Lu-616	47.40	0.11	15.95	7.29	0.17	14.77	9.35	1.18	0.17	0.03	8.10	55.8	7.0	22.2	14.9	0,1	0.0	0,22	0,76
78	2026	50.80	0.08	13.00	8.04	0.17	15.80	10.30	1.00	0,06	0,03	8,93	44,7	16,1	31,6	7,5	0,1	0.0	0.23	0.77
79	1015	46.90	0.25	9,64	10.93	0.16	20.77	8.18	0.68	0.05	0.05	12.15	34.5	14.6	24.2	26.4	0.3	0.0	0.23	0.78
83	1014	49.71	0,06	16,51	5.83	0.13	11.36	12.61	1.76	0.11	0.05	6.48	58.1	20.0	12.3	9.5	0.1	0.0	0.23	0,69
84	Lu2028	50,10	0.10	20.30	5.89	0.10	9.40	11.90	1.80	0,15	0,03	6,55	67,9	9,2	16.8	6,0	0.1	0.0	0.26	0.73
87	1013	47.53	0.17	8.83	9,45	0,22	20,58	8,71	0.44	0.03	0.05	10.50	31.1	17.9	31.8	19.0	0.2	0.0	0.21	0.84
91	1012	49.14	0,05	18.88	5.62	0.11	10.72	12.33	1.61	0.08	0.05	6.25	63.7	13.2	14.3	8.8	0,1	0,0	0,23	0.75
95	1011	49.57	0.06	18.36	5.31	0.11	10.69	13.00	1,53	0,08	0,05	5,90	61,7	16,5	14.6	7.2	0.1	0.0	0.22	0.75
97	Lu2032	50.30	0.05	18,40	5,23	0.10	10.40	11.80	1.90	0.08	0.03	5.81	63.6	13.2	17.5	5.7	0.1	0.0	0 22	0,70
99	1010	49.43	0,09	13.82	7.59	0.15	16.24	9.69	1.02	0.07	0.05	8.44	47.7	12.1	28.9	11.2	0,1	0,0	0,21	0.77
103	1009	47.27	0.08	16.80	6.51	0.11	12.76	11.55	1,36	0,10	0.05	7.23	58.3	14.2	12.8	14.6	0.1	0.0	0.23	0.75
105	2037	50,60	0,01	18.10	4.85	0.11	10.20	12.20	1.60	0,07	0.03	5,39	61,7	14,3	22.9	1.0	0.0	0.0	0.21	0.74
107	1008	49.21	0,12	16.82	6.85	0.14	12.11	11.54	1.45	0.15	0 05	7,61	57,9	14,3	17.8	9,8	0,1	0.0	0.24	0.74
111	1007/1	49,28	0.10	14.80	8.29	0.15	12.80	9.67	1,78	0,12	0.05	9.21	54.7	12.8	21.2	11.2	0.1	0.0	0.27	0.66
113	Lu2039	50.50	0.04	18.00	5,05	0,11	10,40	11.90	1.60	0.08	0.05	5.61	61.6	13.5	23.5	1.5	0.0	0.0	0.22	0.74
116	2041	50.70	0.04	18,40	4,62	0.10	10.10	12.60	1.70	0.07	0.03	5.13	62.5	15.5	19.6	2,4	0,0	0,0	0.21	0.73
118	Lu 617	51.50	0,17	11.70	7.32	0.20	17.93	8.13	1.04	0.16	0,03	8,14	42,0	10.9	41,1	5.9	0.2	0.0	0.19	0.72
118,1	Lu617/1	52,30	0.12	16.55	5.32	0.15	10.81	13.41	1 54	0,05	0,03	5.91	55.7	21.6	22.4	0.1	0.1	0.0	0.22	0.73
119	1005/1	52.89	0.08	16.96	5.74	0.12	6.52	13,11	1.89	0.08	0.05	6.38	59.5	21.3	13.7	0.0	0.1	5.4	0.34	0.68
121	1004	49.82	0.07	17.93	5.85	0.13	10.13	12.64	1.66	0,08	0.05	6.50	61.4	16.6	16.1	5.8	0.1	0.0	0,25	0 73
122	1002/1	48.88	0.09	18.49	6.08	0.13	10.44	12,50	1.49	0.10	0.05	6.76	62.5	14.4	15.0	8.1	0.1	0,0	0.25	0.76
124	1000	49,03	0.09	14.13	6.52	0.12	13.81	10.65	1,15	0,17	0,05	7,25	50.4	16.2	26.6	6.7	0.1	0.0	0.21	0.74
125	Lu2045	48.70	0.06	16,00	5.40	0.11	13.60	10.20	1.40	0.70	0,03	6,00	58,2	12,1	17,1	12,5	0,1	0.0	0.19	0.68

cross-cutting stringers containing disseminated sulfides. Mineralization occurs only at the contacts between the potholes and surrounding rocks. The potholes are filled with fine-grained gabbronorite and norite, poikilitic pyroxenite and norite, spotted anorthosite, troctolite, olivine gabbronorite, anorthositic norite and norite, with fine-grained gabbronorite the most common rocks, locally exhibiting a subaphanitic texture. They are invariably nearly concordant with the layering in the potholes. The occurrence of fine-grained gabbronorite and norite is a distinctive feature of the Lukkulaisvaara intrusion. Fragments of poikilitic pyroxenite and norite form small

TABLE 5. CHEMICAL COMPOSITION OF FINE-GRAINED ROCKS, WITH NORMS, LUKKULAISVAARA INTRUSION

H, m	Sample	SiO_2	TiO_2	Al_2O_3	FeO *	MnO	MgO	CaO	Na_2O	K_2O	P_2O_5	Fe_2O_3	Pl	Cpx	Opx	Ol	Ilm	Qtz	f **	An ***
	Fine-grained rocks from other bodies																			
	146-1	50.35	0.15	11.70	7.14	0.17	13.23	13.50	1.05	0.07	0.03	7.94	41.5	32.1	21.4	4.7	0.2	0.0	0.24	0.73
	146-5	51.90	0.21	15.70	6.03	0.16	9.83	12.85	1.70	0.12	0.03	6.70	55.3	22.4	21.4	0.0	0.3	0.7	0.26	0.69
	146-7	52.15	0.18	16.20	5.40	0.14	10.04	13.34	1.55	0.09	0.04	6.00	55.4	22.4	20.8	0.0	0.2	1.2	0.24	0.72
	146-8	50.20	0.33	13.60	7.42	0.19	12.55	12.35	1.15	0.05	0.06	8.25	47.4	23.5	25.0	3.7	0.4	0.0	0.25	0.75
	k-20-56	48.45	0.13	13.96	7.15	0.27	10.65	13.14	1.75	0.17	0.06	7.95	52.4	28.5	7.6	11.2	0.2	0.0	0.28	0.64
	lu-815	48.02	0.16	14.24	6.11	0.28	11.86	13.70	1.75	0.16	0.04	6.79	52.7	29.8	1.5	15.8	0.2	0.0	0.23	0.65
	lu-80	46.24	0.06	7.12	7.86	0.54	14.87	15.94	0.66	0.10	0.06	8.74	27.2	53.6	0.3	18.8	0.1	0.0	0.24	0.71
	luk1-92	51.21	0.25	12.74	8.81	0.17	18.29	7.18	1.06	0.14	0.06	9.79	44.7	4.8	40.8	9.5	0.3	0.0	0.22	0.74
	luk13-92	52.06	0.08	17.39	4.00	0.12	11.29	13.02	1.54	0.06	0.05	4.44	58.2	18.4	23.3	0.0	0.1	0.0	0.17	0.74
	1luk3-92	40.56	0.11	11.10	10.44	0.17	19.98	12.24	0.12	0.02	0.06	11.60	37.0	18.1	0.0	44.7	0.1	0.0	0.23	0.96
	lu308	51.94	0.15	14.42	6.32	0.14	12.05	12.74	1.95	0.20	0.03	7.02	52.4	25.5	14.1	7.8	0.2	0.0	0.23	0.62
	lu305/2	49.00	0.18	7.50	8.83	0.20	18.65	8.74	0.34	0.08	0.03	9.81	27.1	21.4	46.5	4.7	0.2	0.0	0.21	0.84
	lu303/2	50.35	0.12	7.75	7.87	0.20	18.00	9.70	0.49	0.12	0.03	8.75	28.4	25.1	44.3	2.1	0.2	0.0	0.20	0.78
	lu145-2	53.38	0.09	11.07	8.13	0.17	19.23	6.92	0.85	0.05	0.03	9.03	38.4	6.5	54.2	0.8	0.1	0.0	0.19	0.77
	lu143-2	52.04	0.11	16.77	4.65	0.13	11.10	13.57	1.47	0.07	0.03	5.17	56.1	21.6	21.8	0.4	0.1	0.0	0.19	0.74
	lu613	52.75	0.10	16.28	5.48	0.14	10.75	12.54	1.79	0.07	0.03	6.09	56.3	19.8	23.5	0.0	0.1	0.2	0.23	0.69
	lu612	51.35	0.18	15.95	6.36	0.15	9.79	11.79	1.84	0.11	0.03	7.07	57.3	18.5	23.9	0.0	0.2	0.2	0.27	0.67
	lu854-2	51.82	0.22	15.81	6.29	0.14	14.27	9.11	1.28	0.22	0.08	6.99	54.3	6.6	37.4	1.4	0.3	0.0	0.20	0.74
	lu854-3	52.35	0.25	16.98	5.80	0.13	11.84	9.12	1.70	0.43	0.07	6.45	60.1	6.0	32.9	0.0	0.3	0.6	0.22	0.68
	lu854-6	52.69	0.27	9.42	8.35	0.20	19.59	6.32	0.82	0.14	0.04	9.28	34.5	8.0	56.7	0.5	0.3	0.0	0.20	0.73
	lu854-7	52.48	0.20	13.52	6.93	0.16	16.28	8.11	1.05	0.17	0.03	7.70	46.9	6.8	45.9	0.0	0.2	0.2	0.20	0.75

* FeO as $0.9Fe_2O_3$. ** f: Fe/(Fe + Mg), *** plagioclase composition. Major element as oxides in wt%, normative constituents in vol.%.

disk-shaped inclusions (up to a few cm thick), which usually occur close to the contacts with coarse-grained rocks. Veins of ore-bearing pegmatitic gabbronorite, pyroxenite, as well as their barren equivalents, are represented by massive rocks occurring exclusively within the fine-grained rocks. Relations between the pegmatitic ore-bearing pyroxenite and gabbronorite are ambiguous. It is not unusual to observe that the veins show some zoning: the peripheral parts consist of gabbronorite, whereas the axial parts are represented by pyroxenite. Contacts of the veins with enclosing fine-grained gabbronorite are sharp, and exhibit no evidence of interactions. Bottom zones of the potholes and footwall rocks usually consist of quartziferous gabbroic pegmatites, but “pseudoconglomerates” are a common feature of the pothole bottoms, the “pebbles” consisting of fine-grained gabbronorite or coarse-grained pyroxenite and gabbronorite.

The large bodies (up to 100 m in section) of fine-grained rocks demonstrate a somewhat “autonomous” differentiated series. A vertical section of one of them can be presented as follows: 1) Oikocrystic fine-grained gabbronorite, 2) Equigranular fine-grained pigeonite gabbronorite, gabbro and coarse-grained gabbronorite in the middle part of the body, and 3) Oikocrystic fine-grained gabbronorite. Some bodies of fine-grained rocks have nothing to do with potholes and probably repre-

TABLE 6. CHEMICAL COMPOSITION OF THE PETROCHEMICAL TYPES (CLUSTERS) OF FINE-GRAINED ROCKS, WITH NORMS, LUKKULAISVAARA INTRUSION

Cumulates	Opx + Cpx + Pl			Opx + Pl		
Oxides	1	2	3	4	5	6
SiO_2 wt%	51.85	52.40	52.79	52.64	52.26	53.64
TiO_2	0.17	0.14	0.16	0.24	0.21	0.18
Al_2O_3	16.72	16.31	8.10	16.57	12.78	10.35
FeO	5.30	5.35	8.88	6.11	7.74	8.33
MnO	0.14	0.14	0.21	0.14	0.18	0.19
MgO	11.32	10.82	19.48	13.19	17.68	19.63
CaO	13.38	13.04	9.80	9.21	7.69	6.69
Na_2O	1.02	1.66	0.44	1.51	1.06	0.84
K_2O	0.09	0.09	0.11	0.33	0.16	0.10
P_2O_5	0.03	0.03	0.03	0.08	0.04	0.04
Pl vol.%	54.2	55.9	27.7	57.3	44.5	36.4
Cpx	19.6	21.3	23.3	6.3	7.5	7.2
Opx	24.7	22.3	45.4	36.0	42.8	55.5
Ol	0.0	0.3	3.4	0.1	4.9	0.7
Ilm	0.2	0.2	0.2	0.3	0.2	0.2
Qtz	1.3	0.0	0.0	0.0	0.0	0.0
f*	0.21	0.22	0.21	0.21	0.20	0.20
An**	0.81	0.70	0.81	0.71	0.74	0.75

* f: Fe/(Fe + Mg); ** An: plagioclase composition.

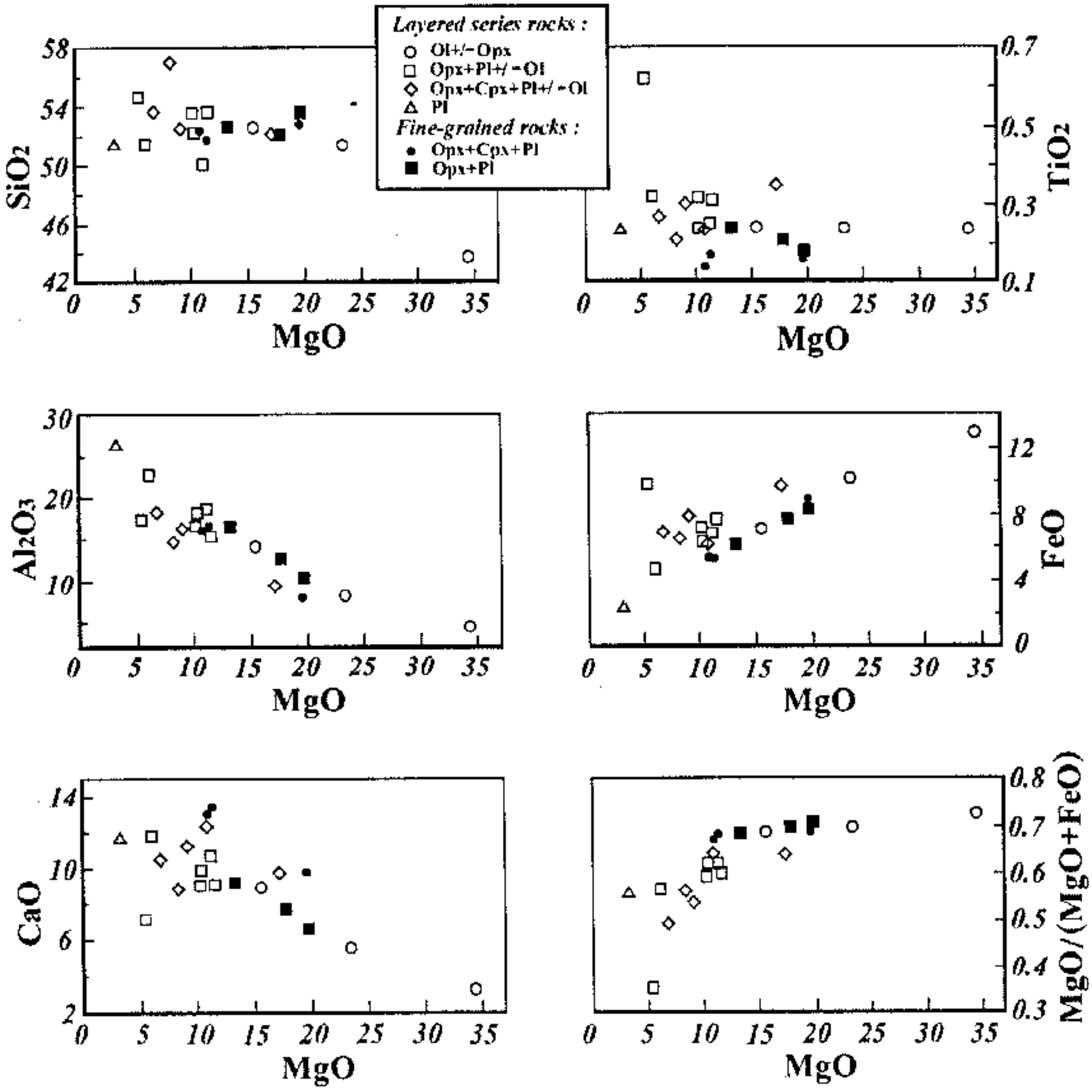

FIG. 5. Comparison of the clusters of the fine-grained and layer-forming rocks. MgO (wt%) *versus* TiO_2, Al_2O_3, FeO, MnO, MgO/(MgO + FeO), CaO, Na_2O, K_2O.

sent fragments of broken sills in the rocks of the layered series (Fig. 3c).

DISTRIBUTION OF MAJOR ELEMENTS ALONG THE VERTICAL SECTION OF THE LUKKULAISVAARA COMPLEX

The distribution of major elements and proportions of normative minerals illustrate the vertical zoning of the Lukkulaisvaara intrusion. Results of 66 chemical analyses of rocks were used; these can be accurately referred to the section along the 1–1, 2–2 and 3–3 profiles (Table 7, Fig. 7). To reveal the regularities in distribution and to eliminate high-frequency fluctuations associated with middle-scale layering, variations in rock composition, and analytical dispersion, the primary data were repeatedly smoothed (Figs. 6a, b).

Olivine was evidently the main mineral of the ultrabasic zone, and is reflected in the pronounced peaks in the distribution of FeO and MgO, and the minima for

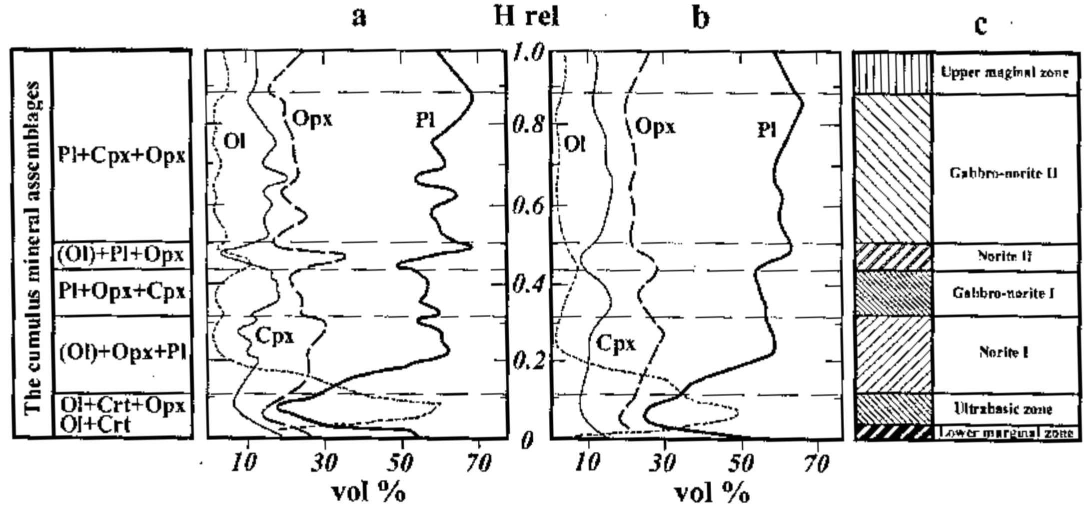

FIG. 6. Cumulate stratigraphy of the Lukkulaisvaara intrusion: normative composition of rocks across the vertical section. a. Two-fold smoothing by the "sliding window" method. b. Ten-fold smoothing by the "sliding window" method; zones clearly defined. c. Vertical section based on cluster analysis and petrographic data (for symbols, see Fig. 2).

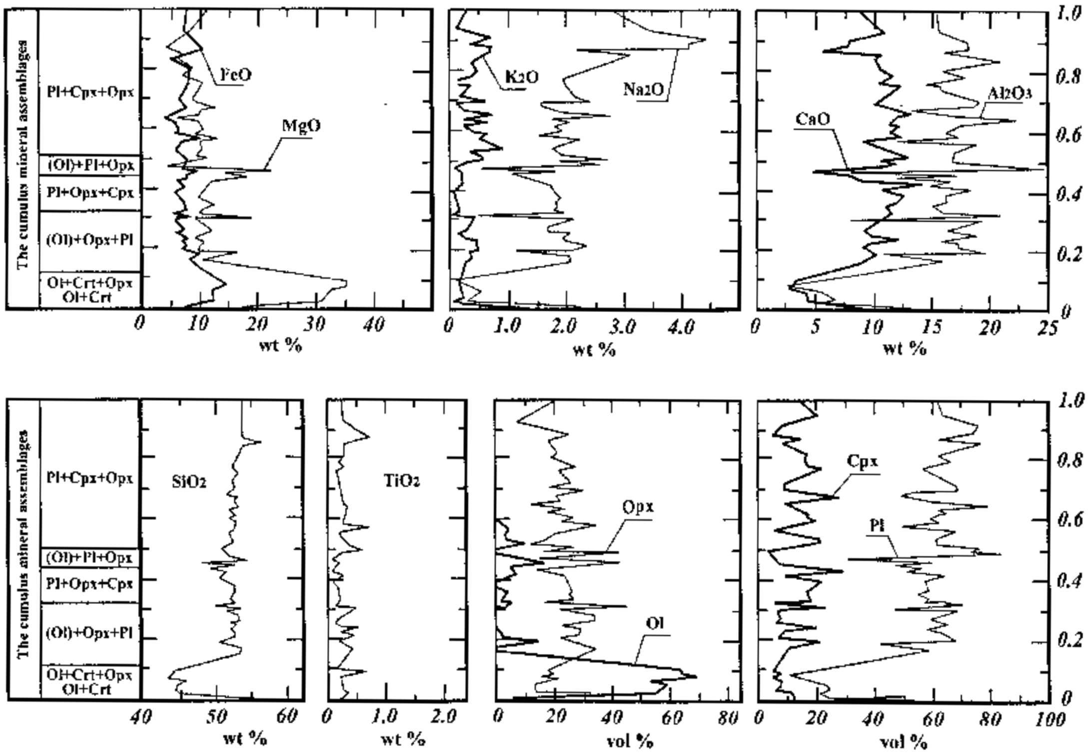

FIG. 7. Distribution of the chemical components and normative minerals across the Lukkulaisvaara intrusion.

TABLE 7. CHEMICAL COMPOSITION OF ROCKS FROM THE LAYERED SERIES, WITH NORMS, LUKKULAISVAARA INTRUSION

N	H, m	H, rel.	Sample	SiO_2	TiO_2	Al_2O_3	FeO *	MnO	MgO	CaO	Na_2O	K_2O	P_2O_5	H_2O	Fe_2O_3	Pl	Cpx	Opx	Ol	Ilm	Qtz	f **	An ***
1	0.0	0.000	108-215	55.40	0.20	14.30	6.29	0.16	7.98	9.55	2.54	0.82	0.01	3.02	6.99	57.7	17.2	19.7	0.0	0.2	5.2	0.31	0.48
2	40.0	0.009	108-140	50.40	0.28	6.25	8.84	0.20	22.30	5.56	0.69	0.20	0.01	4.21	9.82	25.2	12.2	52.8	9.4	0.4	0.0	0.19	0.64
3	100.0	0.022	552/272	40.86	0.31	5.12	11.11	0.18	28.16	5.13	0.28	0.08	0.05	7.06	12.35	20.0	11.9	14.1	53.6	0.4	0.0	0.18	0.81
4	160.0	0.034	552/182	41.97	0.27	6.25	11.62	0.16	29.15	4.23	0.38	0.24	0.04	4.82	12.91	24.3	5.6	14.2	55.5	0.4	0.0	0.18	0.75
5	224.0	0.048	552/86.3	42.20	0.24	5.44	11.58	0.17	30.04	4.11	0.52	0.19	0.04	4.45	12.87	22.1	7.5	12.1	58.0	0.3	0.0	0.18	0.67
6	288.0	0.062	119-166	43.58	0.23	5.10	11.64	0.17	30.10	3.94	0.42	0.20	0.01	4.19	12.94	20.3	7.1	19.8	52.4	0.3	0.0	0.18	0.70
7	345.0	0.074	119-79.7	39.68	0.24	3.70	12.50	0.17	32.13	2.74	0.18	0.20	0.01	7.21	13.89	15.1	4.6	12.9	67.1	0.3	0.0	0.18	0.76
8	395.0	0.085	550/89.0	40.00	0.55	2.45	13.25	0.24	31.73	2.77	0.12	0.08	0.08	7.66	14.72	9.9	7.4	18.7	63.2	0.8	0.0	0.19	0.79
9	440.0	0.095	550/25	40.25	0.13	3.63	11.76	0.17	31.71	2.92	0.16	0.16	0.02	7.52	13.07	14.6	5.4	17.2	62.6	0.2	0.0	0.17	0.79
10	730.0	0.157	102-273	52.40	0.35	14.45	8.09	0.21	11.91	8.57	2.00	0.29	0.01	1.69	8.99	54.6	10.2	34.0	0.8	0.4	0.0	0.28	0.60
11	790.0	0.170	102-179	52.50	0.35	15.60	7.57	0.23	10.08	9.13	2.00	0.38	0.01	1.18	8.41	58.1	10.1	29.9	0.0	0.4	1.5	0.30	0.62
12	880.0	0.189	102-36.6	49.00	0.20	10.50	9.75	0.16	15.89	9.85	1.12	0.28	0.01	2.94	10.84	40.0	21.5	24.4	13.9	0.3	0.0	0.26	0.66
13	910.0	0.196	Lu 601	49.60	0.20	18.90	6.46	0.13	9.43	9.65	2.00	0.46	0.03	3.00	7.18	68.0	5.2	21.0	5.5	0.2	0.0	0.28	0.67
14	973.0	0.209	Lu 602	51.50	0.42	16.80	7.14	0.15	9.86	8.99	2.28	0.39	0.05	3.03	7.94	62.9	7.9	26.8	1.8	0.5	0.0	0.29	0.60
15	1035.0	0.223	Lu 603	51.00	0.26	16.80	6.53	0.15	10.26	9.35	1.91	0.45	0.03	3.02	7.26	61.8	8.2	28.9	0.7	0.3	0.0	0.27	0.64
16	1080.0	0.232	Lu 604	50.25	0.38	15.50	7.59	0.17	9.00	11.48	1.86	0.17	0.04	2.80	8.44	57.2	18.8	22.7	0.8	0.5	0.0	0.33	0.65
17	1160.0	0.249	550/258	51.80	0.15	18.35	5.65	0.10	9.95	9.78	2.00	0.16	0.02	1.24	6.28	64.6	6.1	28.3	0.0	0.2	0.9	0.24	0.68
18	1195.0	0.257	550/206	50.50	0.16	16.75	6.35	0.11	11.50	9.22	1.65	0.25	0.02	2.13	7.06	60.1	6.5	32.2	1.1	0.2	0.0	0.24	0.70
19	1240.0	0.267	Lu 605	51.40	0.18	15.90	6.55	0.10	11.32	8.94	1.56	0.30	0.03	3.27	7.28	57.5	7.1	33.4	0.0	0.2	1.9	0.25	0.69
20	1325.0	0.285	Lu 606	51.05	0.30	17.50	5.83	0.14	9.79	9.45	1.81	0.32	0.04	2.85	6.48	63.0	6.5	28.5	0.0	0.4	1.7	0.25	0.68
21	1388.0	0.298	Lu 607	49.90	0.30	18.65	5.47	0.11	9.14	10.57	2.00	0.39	0.04	2.67	6.08	67.0	9.1	20.4	3.2	0.4	0.0	0.26	0.67
22	1414.0	0.304	Lu 607/1	50.80	0.47	7.85	7.82	0.17	18.19	9.35	0.34	0.06	0.07	4.00	8.69	27.6	22.6	48.1	0.0	0.6	1.1	0.20	0.85
23	1440.0	0.310	Lu 608	49.10	0.13	18.60	5.26	0.12	10.89	9.65	1.74	0.11	0.03	3.41	5.85	65.5	4.2	26.5	3.7	0.2	0.0	0.22	0.72
24	1475.0	0.317	Lu 608/1	48.80	0.19	20.25	5.30	0.12	9.47	11.38	1.84	0.18	0.03	1.46	5.89	69.3	7.7	15.4	7.3	0.2	0.0	0.24	0.73
25	1499.0	0.322	Lu 609	51.90	0.20	15.70	6.42	0.18	11.27	11.28	1.78	0.14	0.03	0.41	7.13	55.8	16.7	25.8	1.5	0.2	0.0	0.25	0.67
26	1553.0	0.334	Lu 610	51.60	0.18	15.75	7.25	0.16	10.76	11.28	1.83	0.10	0.03	0.58	8.06	56.1	16.7	24.6	2.4	0.2	0.0	0.28	0.67
27	1613.0	0.347	Lu 611	50.95	0.16	14.70	6.84	0.16	12.00	10.57	1.77	0.15	0.03	2.04	7.60	53.9	16.4	25.6	3.9	0.2	0.0	0.25	0.65
28	1705.0	0.367	Lu 612	51.35	0.18	15.95	6.42	0.15	9.79	11.79	1.84	0.11	0.03	2.05	7.13	57.3	18.5	24.0	0.0	0.2	0.1	0.27	0.67
29	1805.0	0.388	Lu 613	52.15	0.10	16.10	5.47	0.14	10.63	12.70	1.77	0.07	0.03	0.51	6.08	56.1	20.9	22.3	0.5	0.1	0.0	0.23	0.69
30	1915.0	0.412	Lu 614	49.30	0.23	17.95	6.86	0.14	11.05	10.16	1.68	0.23	0.03	1.72	7.62	62.9	7.6	22.1	7.2	0.3	0.0	0.26	0.71
31	1979.0	0.426	Lu 615	50.05	0.15	14.05	5.88	0.17	11.42	13.72	1.45	0.21	0.03	2.19	6.54	50.5	29.1	14.3	5.9	0.2	0.0	0.23	0.69
32	2040.0	0.439	Lu 616	47.40	0.11	15.95	7.29	0.17	14.77	9.35	1.18	0.17	0.03	2.56	8.10	55.8	7.0	22.2	14.9	0.1	0.0	0.22	0.76
33	2081.0	0.448	Lu 617	51.50	0.17	11.70	7.32	0.20	17.93	8.13	1.04	0.16	0.03	0.83	8.14	42.0	10.9	41.1	5.9	0.2	0.0	0.19	0.72
34	2116.0	0.455	Lu 618	46.50	0.30	16.65	8.40	0.15	14.32	8.84	1.59	0.21	0.03	2.38	9.33	59.8	4.9	13.3	21.6	0.4	0.0	0.25	0.71
35	2176.0	0.468	Lu 619	53.25	0.08	7.85	9.54	0.19	21.77	4.83	0.55	0.09	0.03	0.39	10.60	28.3	4.4	67.2	0.1	0.1	0.0	0.20	0.77
36	2240.0	0.482	Lu 622	51.16	0.25	24.00	3.93	0.06	4.72	10.72	2.50	0.29	0.05	1.30	4.37	81.5	0.0	15.7	0.0	0.3	2.4	0.32	0.69
37	2283.0	0.491	Lu 623	49.90	0.13	20.80	5.44	0.08	9.12	9.60	1.82	0.34	0.03	0.98	6.05	71.7	0.0	26.7	1.5	0.2	0.0	0.25	0.72
38	2307.0	0.496	Lu 304	50.05	0.57	20.45	5.66	0.14	5.31	11.48	2.60	0.55	0.11	1.79	6.29	74.5	11.1	11.5	2.2	0.7	0.0	0.38	0.62
39	2364.0	0.508	Lu305/1	49.20	0.36	16.55	7.23	0.13	10.82	10.36	1.87	0.50	0.07	2.85	8.04	61.0	12.7	16.0	9.8	0.4	0.0	0.28	0.64
40	2406.0	0.517	Lu 306	50.30	0.38	16.45	6.15	0.15	9.09	12.70	1.83	0.33	0.04	1.19	6.83	59.3	21.3	15.6	3.3	0.5	0.0	0.28	0.66
41	2490.0	0.535	Lu 307	50.65	0.26	16.45	5.68	0.13	9.57	11.78	1.69	0.75	0.03	1.42	6.31	60.3	18.3	18.5	2.6	0.3	0.0	0.25	0.64
42	2603.0	0.560	Lu 309	49.60	0.21	17.90	6.69	0.12	9.53	8.84	2.09	0.50	0.03	3.63	7.43	66.7	4.7	24.0	4.3	0.3	0.0	0.29	0.64
43	2658.0	0.572	Lu 310	50.70	0.61	12.30	9.65	0.16	12.32	8.74	1.48	0.57	0.09	3.06	10.73	48.2	14.8	33.9	2.4	0.8	0.0	0.31	0.60
44	2720.0	0.585	Lu 311	51.00	0.23	16.80	5.79	0.13	9.01	12.14	1.87	0.31	0.03	1.73	6.43	60.4	18.5	20.5	0.4	0.3	0.0	0.27	0.66
45	2783.0	0.598	Lu 312	51.70	0.19	16.10	6.18	0.15	10.54	11.33	1.74	0.23	0.03	2.23	6.87	57.3	16.2	26.2	0.0	0.2	0.0	0.25	0.68
46	2858.0	0.615	Lu 313	50.60	0.27	16.90	5.51	0.14	9.67	11.53	2.00	0.57	0.03	2.51	6.12	62.1	16.9	15.8	4.8	0.3	0.0	0.25	0.62
47	2899.0	0.623	Lu 314	52.60	0.31	17.40	5.89	0.13	9.77	11.28	1.74	0.25	0.05	1.00	6.55	60.1	13.0	24.6	0.0	0.4	1.8	0.26	0.69
48	2967.0	0.638	Lu 315	51.10	0.32	21.90	3.93	0.09	5.87	11.63	2.60	0.70	0.03	1.88	4.37	77.4	8.7	11.4	2.1	0.4	0.0	0.28	0.63
49	3013.0	0.648	Lu 316	51.90	0.25	16.70	5.14	0.11	9.77	11.53	1.83	0.33	0.03	2.16	5.71	59.7	16.1	22.7	0.0	0.3	1.1	0.23	0.66
50	3075.0	0.661	Lu 317	52.30	0.23	15.80	5.93	0.15	9.48	13.06	1.74	0.17	0.03	1.62	6.59	55.6	23.1	19.9	0.0	0.3	1.1	0.26	0.68
51	3122.0	0.671	Lu 318	51.60	0.23	13.10	7.34	0.20	11.68	12.19	1.52	0.21	0.03	1.97	8.16	48.0	25.5	24.5	1.7	0.3	0.0	0.27	0.66
52	3182.0	0.684	Lu 319	51.50	0.19	14.50	6.57	0.16	11.53	11.07	1.52	0.12	0.03	1.96	7.30	52.1	17.9	29.0	0.0	0.2	0.8	0.25	0.69
53	3207.0	0.690	Lu 321	49.85	0.20	18.00	6.39	0.15	9.36	9.70	2.28	0.53	0.03	2.84	7.10	67.1	8.5	17.1	7.1	0.2	0.0	0.28	0.61
54	3278.0	0.705	Lu 322	51.80	0.21	18.90	6.24	0.15	8.55	10.52	2.09	0.17	0.03	1.15	6.94	66.1	8.1	24.7	0.0	0.2	0.9	0.30	0.68
55	3448.0	0.742	Lu 323	50.80	0.20	15.70	7.01	0.19	9.78	11.23	1.96	0.31	0.03	2.12	7.79	58.1	17.8	20.6	3.2	0.2	0.0	0.29	0.63
56	3509.0	0.755	Lu 324	51.70	0.14	15.30	6.97	0.20	9.92	11.84	1.91	0.20	0.03	1.99	7.75	55.8	20.4	22.3	1.3	0.2	0.0	0.29	0.64
57	3544.0	0.762	Lu 325	51.90	0.26	14.30	8.04	0.18	10.28	10.26	2.00	0.35	0.03	2.19	8.94	54.5	17.3	27.1	0.8	0.3	0.0	0.31	0.59
58	3645.0	0.784	Lu 326	51.40	0.20	17.60	7.07	0.18	7.41	11.48	2.23	0.44	0.03	2.27	7.86	64.4	15.7	18.7	1.0	0.2	0.0	0.35	0.62
59	3745.0	0.805	Lu 10/1	46.79	0.24	14.14	7.76	0.14	7.56	9.31	2.27	0.31	0.03	10.12	8.62	60.3	16.2	20.1	3.0	0.3	0.0	0.37	0.55
60	3915.0	0.842	Lu 10/2	51.78	0.28	20.14	6.12	0.11	4.91	9.82	3.00	0.55	0.03	2.10	6.80	75.5	6.8	16.5	0.0	0.3	0.9	0.42	0.57
61	3975.0	0.855	Lu 10/4	52.68	0.39	16.28	8.72	0.16	6.33	10.30	2.13	0.63	0.03	0.90	9.69	61.3	14.2	20.5	0.0	0.5	3.5	0.44	0.59
62	4035.0	0.868	207-7/?	54.23	0.66	15.68	10.02	0.21	5.51	5.63	4.00	0.69	0.05	1.78	11.14	69.2	4.1	24.8	0.0	0.8	1.2	0.51	0.36
63	4085.0	0.878	Lu 237	51.98	0.68	17.60	9.87	0.12	4.43	7.48	3.95	0.33	0.06	2.52	10.97	73.2	6.1	17.4	2.4	0.8	0.0	0.56	0.44
64	4185.0	0.900	Lu74/457	51.92	0.46	17.53	8.39	0.18	5.46	7.70	4.20	0.65	0.06	1.82	9.32	74.5	8.7	7.2	9.1	0.5	0.0	0.47	0.39
65	4335.0	0.932	Lu 74/440	51.85	0.24	15.15	6.99	0.17	7.94	10.44	3.28	0.10	0.03	3.67	7.77	62.0	20.1	12.8	4.8	0.3	0.0	0.34	0.47
66	4650.0	1.000	8942-2/?	51.30	0.22	14.75	7.16	0.18	10.63	8.48	2.58	0.30	0.01	3.30	7.96	59.2	11.4	25.0	4.0	0.3	0.0	0.28	0.53

* FeO as $0.9Fe_2O_3$. ** f: Fe/(Fe + Mg), ***: plagioclase composition. Major element as oxides in wt%, normative constituents in vol.%.

SiO_2, CaO, Al_2O_3 and Na_2O. An increase of normative plagioclase and orthopyroxene, and SiO_2, CaO, Al_2O_3 and Na_2O concentrations, marks the appearance of cumulative plagioclase and a slight increase of orthopyroxene in the norite-1 zone. An increase in normative clinopyroxene and CaO concentrations and slight decrease of the cumulative and normative orthopyroxene content, and MgO, Al_2O_3 concentrations, mark the appearance of cumulative clinopyroxene in the gabbronorite-1 zone. An increase in normative olivine and MgO concentrations, and slight decrease in SiO_2, CaO, Al_2O_3 and Na_2O concentrations, mark the appearance of cumulative olivine at the bottom of the gabbronorite-1 zone. Orthopyroxene and plagioclase as cumulus minerals characterize the norite-2 zone, whereas olivine occurs at the bottom of the zone, and clinopyroxene occurs as an intercumulus mineral. These changes are reflected by the distribution curves of normative orthopyroxene, plagioclase, olivine and clinopyroxene. The decrease in clinopyroxene content is accompanied by an increase of MgO and lower CaO concentrations. The gabbronorite-2 zone is characterized by the presence of orthopyroxene, clinopyroxene and plagioclase as cumulus minerals. An increase in clinopyroxene content is accompanied by an increase of CaO and decrease of MgO. The presence of normative olivine in these rocks is an artifact, since magnetite was not considered in our calculations. Exclusion of magnetite from the calculations of normative composition was conditioned by analytical difficulties in determining ferric and ferrous iron, their dependence on the degree of the rock alteration, and probable changes during sample grinding. Total iron content is presented as FeO, which is the most appropriate for direct comparison of the chemical composition of the rocks with the results of modeling (Frenkel *et al.* 1988, 1989). The upper boundary of this zone and the layered series, as a whole, corresponds to rocks with maximum P_2O_5 and TiO_2 contents and a slight increase in normative quartz content. A sharp decrease in P_2O_5 and TiO_2 concentrations further upward is a characteristic feature of the lower 200 m of the upper marginal zone. The presence of normative olivine in these rocks also is an artifact.

According to the chemical data (Table 7) we calculated the mean composition of the layered complex (in wt%): 51.02% SiO_2, 0.28% TiO_2, 15.35% Al_2O_3, 7.82% FeO, 0.16% MnO,12.69% MgO, 9.61%CaO, 2.00% Na_2O, 0.33% K_2O, and 0.03% P_2O_5. The wide occurrence of the layered series and its constant thickness suggest that the calculated composition may be close to that of the initial magma if emplacement of a single magma formed the massif.

Judging from the cumulate sequence within the layered series, the order of crystallization (ignoring the autonomous series of potholes) was as follows: olivine + chromian spinel → olivine + chromian spinel + orthopyroxene → olivine + orthopyroxene + plagioclase → orthopyroxene + plagioclase + clinopyroxene → plagioclase + olivine + orthopyroxene → orthopyroxene + plagioclase → orthopyroxene + clinopyroxene + plagioclase + olivine → orthopyroxene + clinopyroxene + plagioclase. The olivine-bearing cumulates invariably overlie the pothole structures. The presence of fine-grained gabbronorite and norite is a typical feature of the potholes of the Lukkulaisvaara intrusion. Their origin may be explained by injections of new batches of magma. Thus the distribution of elements along the vertical sequence of the largest lenticular bodies of fine-grained rocks is very revealing.

The first body

Concentrations of the major elements were determined in 24 samples collected from the first-described body of fine-grained gabbronorite (Figs. 2, 3a). The real thickness of the body is about 90 m. Distributions of the major elements and normative minerals are very simple (Fig. 8a, Table 5), and the weighted mean composition of the body is (wt%) 51.88% SiO_2, 0.17% TiO_2, 16.74% Al_2O_3, 5.35% FeO, 0.14% MnO, 11.20% MgO, 13.33% CaO, 1.06% Na_2O, 0.09% K_2O and 0.03% P_2O_5.

The second body

Concentrations of the major elements were determined in 32 samples collected from the second-described body of fine-grained rocks (Fig. 2). The real thickness is about 100 m. Patterns of distribution of the major elements and normative minerals are more complicated than in the first body (Fig. 8c, Table 5). The absence of modal olivine in the fine-grained lithologies (the parental melt was olivine-saturated) may be due to rapid crystallization, but in the axial part of the body, olivine was found in coarse-grained norites. The weighted mean composition of the body is (wt%) 50.97% SiO_2, 0.10% TiO_2, 15.75% Al_2O_3, 6.81% FeO, 0.14% MnO, 12.32% MgO, 12.20% CaO, 1.54% Na_2O, 0.13% K_2O, and 0.04% P_2O_5. The weighted mean composition of the Lukkulaisvaara intrusion is chemically close to that of the lenticular bodies of fine-grained rocks, but there are some differences in Ca content.

DISTRIBUTION OF Ni, Co, Cr AND Cu ALONG THE VERTICAL SEQUENCE OF THE LUKKULAISVAARA MASSIF AND BODIES OF FINE-GRAINED ROCKS; CONCENTRATIONS OF THE LREE IN THE FINE-GRAINED ROCKS

The entire Lukkulaisvaara section

The maximum Cr concentration was observed in the ultrabasic zone, where chromian spinel is a cumulus mineral (Fig. 9). Cr contents in the basic part of the intrusion coincide with the marker horizons of potholes and the bodies of fine-grained rocks, where disseminations of chromian spinel were found. A relatively dis-

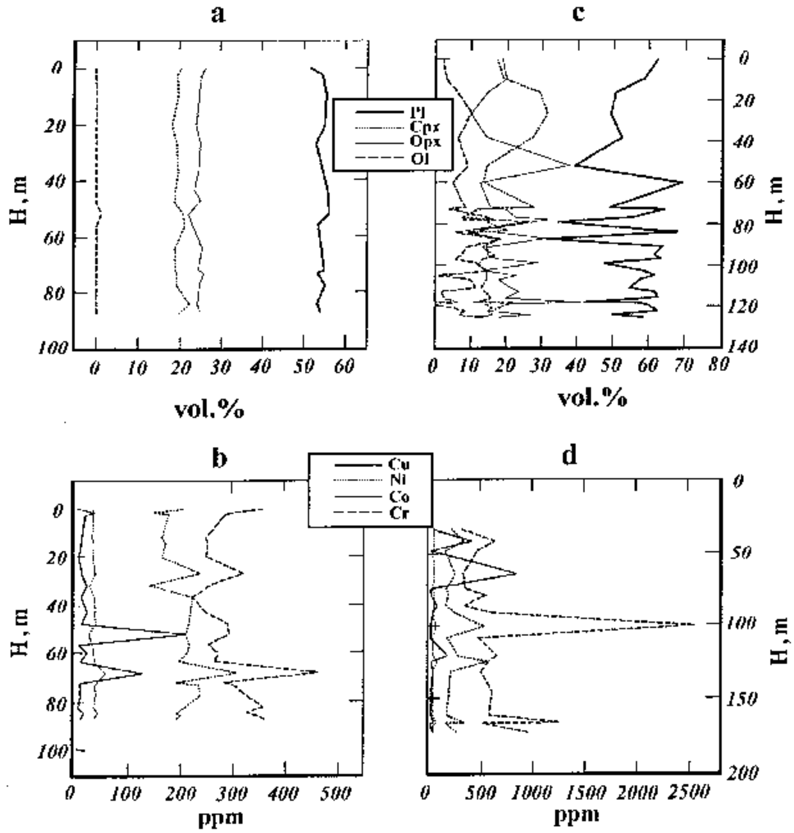

FIG. 8. Distribution of the normative minerals and Cu–Ni–Co–Cr across the bodies of fine-grained rocks: (a, b): first body, and (c, d): second body.

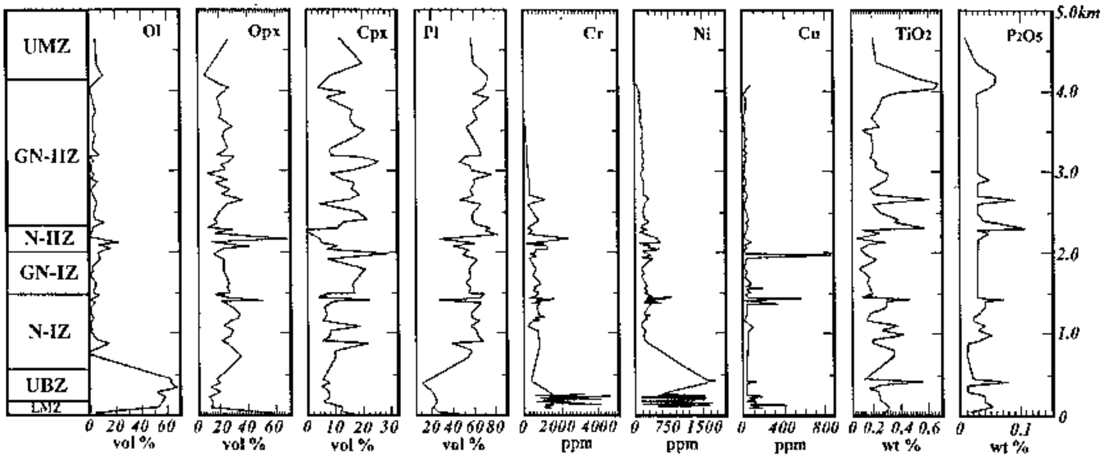

FIG. 9. Distribution of normative minerals and Ni, Co, Cr, Cu across the Lukkulaisvaara intrusion.

tinct correlation between Cr and Ni is observed in the basic part of the intrusion. Ni distribution correlates with the content of olivine and Fe–Ni–Cu sulfide. The distribution of Cu is not related to the rock-forming minerals. Low concentrations and uniform distribution of Cu were observed in the norite-1 zone, gabbronorite-1 zone, norite-2 zone and gabbronorite-2 zone, but high concentrations of Cu were observed in the ultrabasic zone and at the boundaries between norite-1 and gabbronorite-1 zones, gabbronorite-1 and norite-2 zones. The maximum Cu content in the basic part of intrusion coincides with the marker horizons in the footwall units, with Fe–Ni–Cu sulfides developed around potholes.

Table 8 gives the weighted mean content of Ni (373 ppm), Co (54 ppm), Cr (514 ppm) and Cu (46 ppm) within the massif as a whole. The Ni/Co ratio decreases regularly up the profile, in agreement with the conclusion that fractional crystallization was important in magma evolution, because the partition coefficients of Co between the ferromagnesian minerals and the melt are less than those of Ni. The significance of fractional crystallization in the distribution of trace elements is confirmed by the evolution of their concentrations in residual melts. These concentrations were calculated as weighted average values for the interval from the level of sampling to the lower boundary of the upper marginal zone. During solidification of the complex, constant convection of the magma occurred above the upper boundary of the cumulates, so the weighted mean concentrations might be considered to be the content of the elements in the residual magma. The evolution of relative concentrations of trace elements in comparison to Ti and P behavior is illustrated by Figure 10. Ti and P may be considered as incompatible elements, because cumulate magnetite and apatite were not formed during crystallization. The deflection of Ni and Cr evolution curves from those for Ti and P took place at the very beginning of crystallization, because olivine and chromite were the first liquidus phases. However, Cr behavior is more complicated and related to the influence of the fine-grained rocks, which are widespread in the gabbronorite-2 zone. Evolutionary paths of Cu deviate significantly from those of Ti and P from the point at which sulfide phases appeared. After that, Cu behaves as a typical incompatible element.

The lenticular bodies of fine-grained gabbronorite and norite

In the first body (Table 9, Fig. 8b), Cr concentrations in the fine-grained rocks are generally above 250 ppm and show a symmetrical distribution along the vertical sequence. Relatively Cr-rich rocks (460 ppm) were found in the sulfide-bearing altered coarse-grained gabbronorite (the axial part of the body). The distribution of Cr is in agreement with the clinopyroxene composition (Cr content in the clinopyroxene is up to 0.70 wt% Cr_2O_3 at the bottom and top of the body, and up to 0.17 wt% near the axial part). As shown in Figure 8, the distribution of Ni and Co is similar. The maximum content of these elements (306 ppm Ni, 57 ppm Co) was found in the sulfide-bearing rocks. The weighted mean contents of the elements in the first body are: 288 ppm Cr, 205 ppm Ni, 38 ppm Co, 31 ppm Cu.

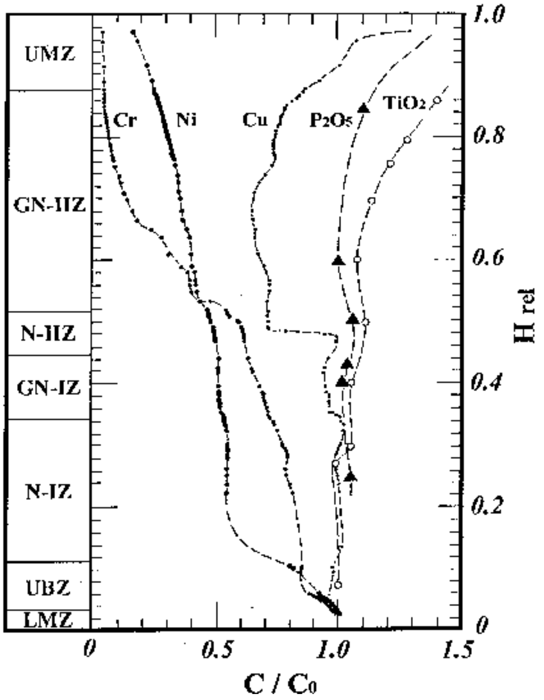

FIG. 10. Variation of relative concentrations of Cu, Ni, Cr, P_2O_5, TiO_2 in the residual magma. C is content of corresponding element in the residual magma, and C_0, in the initial magma.

In the second body (Table 9, Fig. 8d), the highest Cr content is found in the chromian-spinel-bearing fine-grained pyroxenites at the bottom (up to 2600 ppm) and at the top (500–1250 ppm) of the body. Ni concentration is related to the olivine and in some cases to the Fe–Ni–Cu sulfide content. The maximum content of this element (550 ppm) is found in the olivine-bearing coarse-grained norites at the axial part of the body of fine-grained rocks. The distribution of Cu shows no dependence on the rock-forming silicate content. Slightly higher concentrations and a uniform distribution of Cu are noted in the fine-grained pyroxenites with fine sulfide grains. The weighted mean contents of the elements in the second body are: 856 ppm Cr, 287 ppm Ni, 53 ppm Co, and 75 ppm Cu.

Three total rare-earth element (ΣREE) concentrations in the fine-grained rocks were obtained (Table 10). The first two patterns apply to fine-grained norite, the

TABLE 8. Cu–Ni–Co–Cr CONCENTRATIONS IN VARIOUS ROCK-TYPES FROM THE LAYERED SERIES, LUKKULAISVAARA INTRUSION

N	Sample	H m	H rel	Cu	Ni	Co	Cr	Ni/Co
1	552/284	95	0.023	177	1180	98	934	12.04
2	552/281	97	0.024	39	1219	920	382	1.33
3	552/256	112	0.027	41	1125	91	973	12.36
4	552/238	125	0.031	100	493	600	592	0.82
5	552/230	129	0.032	78	1150	1070	571	1.07
6	552/228	130.5	0.032	407	1692	1300	152	1.30
7	552/227	131.2	0.032	99	142	210	518	0.68
8	552/225	132.6	0.032	100	1311	1220	470	1.07
9	552/221	135	0.033	112	1163	1020	184	1.14
10	552/221	135.3	0.033	52	1074	1030	229	1.04
11	552/216	138.2	0.034	117	129	300	33	0.43
12	552/201	148	0.036	105	1235	910	436	1.36
13	552/189	155.2	0.038	81	1665	118	727	14.11
14	552/182	160	0.039	118	1324	820	358	1.61
15	552/172	166.6	0.041	98	225	37	486	6.08
16	552/167	170.1	0.042	114	213	38	663	5.61
17	552/165	172	0.042	94	890	790	217	1.13
18	552/161	174.7	0.043	61	1114	1180	391	0.94
19	552/154	179	0.044	10	766	138	989	5.55
20	552/149	183	0.045	104	616	710	647	0.87
21	552/139	190	0.047	27	1314	1160	202	1.13
22	552/131	195	0.048	103	1501	1240	25	1.21
23	552/126	198	0.048	90	1435	1400	691	1,03
24	552/104	212	0,052	87	1336	1310	226	1.02
25	552/94	218.8	0.054	74	1385	1160	825	1,19
26	552/93.5	219.1	0,054	117	120	21	722	5.71
27	552/93	219.5	0,054	107	1555	1070	426	1.45
28	552/86.3	224	0,055	29	1512	1310	260	1.15
29	552/85.5	224.6	0.055	41	1311	1190	510	1.10
30	552/75	232	0.057	63	1083	1170	190	0.93
31	552/73.1	233,2	0,057	105	1193	1100	152	1.08
32	552/71	234.6	0.057	58	990	980	73	1.01
33	552/70.9	234.7	0.057	69	472	860	979	0.55
34	552/69	236	0.058	163	1547	1590	757	0.97
35	552/62.7	240,1	0.059	72	847	990	745	0.86
36	552/62,5	240.2	0.059	70	1340	110	427	12.18
37	552/56	244.5	0.06	53	857	1160	920	0.74
38	552/55.3	245	0.06	20	546	700	490	0.78
39	550/89,0	395	0.097	14	1587	131	379	12.11
40	550/53.6	420	0.103	44	1579	122	175	12.94
41	550/52.6	421	0.103	110	1724	144	299.6	11.97
42	550/45	425.8	0.104	34	1575	135	290	11.67
43	550/35	432	0.106	24	1599	133	285	12.02
44	Lu 601	910	0.223	41	202	37	791	5.46
45	Lu 602	973	0.238	49	170	41	720	4.15
46	Lu 603	1035	0,253	49	210	42	705	5.0
47	Lu 604	1080	0.264	68	143	42	94	3.40
48	550/258	1160	0.284	10	146	49	478	2.98
49	550/246	1168	0.286	15	254	59	772	4,31
50	550/206	1195	0.293	10	188	55	546	3.42
51	550/186	1208.5	0.296	10	323	550	104	0.59
52	550/166	1222	0.299	15	232	39	756	5.95
53	550/146	1235.5	0,302	14	228	45	755	5,07
54	Lu 605	1240	0.304	27	194	47	800	4.13
55	Lu 606	1325	0.324	32	258	40	678	6.45
56	Lu 654	1364	0.334	27	328	52	756	6.31
57	Lu 653	1372	0.336	29	175	46	740	3,80
58	Lu 652	1374	0,336	114	370	41	578	9.02
59	Lu 651	1380	0.338	310	640	69	767,1	9.28
60	Lu 650	1384	0.339	34	313	46	401	6.80
61	Lu 649	1387	0.34	175	172	35	325.9	4.91
62	Lu 607	1388	0.34	41	211	36	633	5,86
63	Lu 607/1	1414	0.346	14	367	630	584	0.58
64	Lu 631	1425	0.349	305	655	42	408	15.60
65	Lu 632	1435	0.351	72	297	33	273	9.0
66	Lu 608	1440	0.353	43	244	43	961	5.67
67	Lu 608/1	1441	0,353	322	403	43	348,4	9.37
68	Lu 633	1441.3	0.353	547	816	68	332.4	12,0
69	Lu 634	1446	0.354	44	410	42	363	9.76
70	Lu 635	1480	0.362	38	270	49	748	5.51
71	Lu 609	1499	0.367	26	190	41	724	4,63
72	Lu 636	1509	0.369	68	280	43	638	6,51
73	Lu 637	1520	0.372	56	225	43	553	5.23
74	Lu 638	1540	0.377	24	200	46	523	4.35
75	L 610	1553	0.38	30	188	43	584	4.37
76	Lu 639	1558	0.381	178	255	42	503	6.07
77	Lu 640	1571	0.385	28	240	52	513	4.62
78	Lu 611	1613	0.395	73	232	45	888	5.16
79	Lu 612	1705	0.417	17	140	42	500	3.33
80	Lu 641	1735	0.425	24	200	33	492	6.06
81	Lu 613	1805	0.442	12	139	35	634	3.97
82	Lu 614	1915	0.469	23	382	58	333	6.59
83	Lu 642	1935	0.474	38	193	50	292	3.86
84	Lu 643	1936	0.474	38	163	51	327	3.20
85	Lu 644	1956	0.479	403	340	55	631.2	6.18
86	Lu 615	1979	0.484	844	250	50	327.5	5,0
87	Lu 645	1994	0.488	22	187	50	542	3.74
88	Lu 646	2006	0.491	36	255	36	608	7.08
89	Lu 616	2040	0.499	18	551	71	564	7,76
90	Lu 235	2045	0.501	36	310	390	292	0.79
91	Lu 617	2081	0,509	36	326	630	246	0.52
92	Lu 617/1	2091	0.512	10	156	39	508	4.0
93	Lu 647	2102	0.515	9	304	550	38	0,55
94	Lu 648	2110	0,517	28	70	11	103	6.36
95	Lu 618	2116	0,518	62	581	81	205	7.17
96	Lu 619	2176	0.533	6	474	980	394	0,48
97	Lu 622	2240	0.548	26	110	20	208	5.5
98	Lu 623	2283	0.559	29	266	29	420	9,17
99	Lu 304	2307	0,565	43	103	35	177	2.94
100	Lu 305/1	2364	0.579	42	309	51	498	6.06
101	Lu 306	2406	0.589	46	198	36	821	5,5
102	Lu 307	2490	0,61	44	157	33	521	4.76
103	Lu 309	2603	0.637	23	194	40	192	4.85
104	Lu 310	2658	0.651	27	316	510	167	0.62
105	Lu 311	2720	0.666	43	169	36	273	4.69
106	Lu 312	2783	0,681	17	192	43	318	4.47
107	Lu 313	2858	0.7	23	169	33	222	5,12
108	Lu 314	2899	0.71	20	169	39	256	4.33
109	Lu 315	2967	0.726	6	103	25	101	4.12
110	Lu 316	3013	0.738	7	176	31	159	5.68
111	Lu 317	3075	0.753	12	162	40	157	4.05
112	Lu 318	3122	0.764	28	204	41	159	4.98
113	Lu 331	3142	0.769	35	174	34	103	5.12
114	Lu 332	3150	0.771	35	186	34	93	5.47
115	Lu319	3182	0,779	32	136	50	115	2.72
116	Lu 333	3193	0.782	40	165	39	83	4.23
117	Lu 320	3200	0.783	8	159	37	110	4.30
118	Lu 334	3205	0.785	15	154	30	88	5,13
119	Lu 321	3207	0.785	20	155	28	75	5,54
120	Lu 335	3220	0.788	38	165	38	68	4.34
121	Lu 336	3231	0.791	38	178	38	73	4,68
122	Lu 337	3253	0.796	17	170	43	73	3.95
123	Lu 322	3278	0.802	26	137	36	55	3.81
124	Lu 338	3288	0.805	22	158	42	48	3.76
125	Lu 354	3312	0.811	28	149	49	79	3,04
126	Lu 349	3342	0.818	17	129	40	56	3.23
127	Lu 348	3362	0,823	22	188	47	83	4.0
128	Lu 347	3381	0.828	18	117	45	72	2.6
129	Lu 346	3396	0.831	34	117	36	58	3.25
130	Lu 345	3406	0.834	40	99	30	49	3.3
131	Lu 344	3412	0.835	22	180	47	103	3,83
132	Lu 343	3423	0.838	22	134	47	72	2,85
133	Lu 323	3448	0.844	27	155	47	31	3.30
134	Lu 339	3474	0.85	21	138	47	27	2,94
135	Lu 340	3487	0.854	17	130	46	23	2.83
136	Lu 324	3509	0.859	7	149	42	40	3.55
137	Lu 353	3528	0,864	20	120	49	23	2,45
138	Lu 325	3544	0,868	15	156	50	27	3.12
139	Lu 341	3545	0.868	18	158	57	29	2.77
140	Lu 342	3546	0,868	15	190	120	25	1.58
141	Lu 352	3549	0.869	10	116	55	34	2.11
142	Lu 350	3568	0.873	32	140	49	35	2.86
143	Lu 351	3589	0.879	18	110	43	17	2.56
144	Lu 326	3645	0.892	15	116	44	28	2.64
145	Lu 10/1	3745	0.917	37	115	56	28	2.05
146	Lu 10/2	3915	0.958	37	70	37	19	1.89
147	Lu 10/4	3975	0.973	18	94	51	28	1.84
148	Lu 237	4085	1	85	24	45	15	0.53

Concentrations are reported in ppm.

TABLE 9. Cu, Ni, Co, Cr CONTENT IN THE FINE-GRAINED ROCKS, LUKKULAISVAARA INTRUSION

Sample	H m	Ni	Co	Cr	Cu	Sample	H m	Ni	Co	Cr	Cu
First body						**Second body**					
1505	0.3	206	38	354	17	Lu-2004	33.0	220	45	320	47
1506	1.5	150	30	307	40	Lu 644	41.0	340	55	631	403
1507	2.4	180	38	287	22	Lu-2006	48.0	157	37	461	19
1508	12.1	167	35	249	14	Lu 615	64.0	250	50	327	844
1509	14.1	173	39	254	14	Lu-2012	74.0	168	41	351	15
1510	20.1	167	36	250	10	Lu 645	79.0	187	50	542	22
1511	27.1	238	42	320	16	Lu-2016	86.0	162	53	338	79
1512	31.8	144	30	257	25	Lu 646	91.0	255	36	608	36
1513	36.8	225	39	224	14	Lu-2019	100.0	524	67	2554	17
1514	42.8	220	40	247	25	Lu-2021	108.0	169	40	474	14
1515	47.7	217	41	290	15	Lu-2025	121.0	276	42	651	175
1516	52.0	210	29	293	210	Lu 616	125.0	551	71	564	18
1517	56.3	217	35	254	10	Lu-2028	132.0	206	40	492	41
1518	60.0	214	37	271	24	Lu-2032	145.0	184	40	599	16
1519	63.8	197	39	267	13	Lu-2039	161.0	172	42	569	17
1520	68.5	306	57	462	127	Lu 617	166.0	326	63	1246	36
1521	72.3	194	40	284	13	Lu 617/1	166.5	156	39	508	10
1522	73.2	234	39	301	12	Lu-2045	173.	262	38	955	35
1523	77.5	237	40	324	12						
1524	82.2	207	37	357	7						
1525	84.2	194	43	327	19						
1526	85.5	200	39	347	14						
1527	87.0	190	37	360	11						

H m: height in meters. Concentrations are reported in ppm.

TABLE 10. COMPOSITION OF FINE-GRAINED ROCKS FROM VARIOUS UNITS, LUKKULAISVAARA INTRUSION

Sample	SiO_2	TiO_2	Al_2O_3	Fe_2O_3	MnO	MgO	CaO	Na_2O	K_2O	P_2O_5	Total
1(92)	51.08	0.25	12.71	9.05	0.17	18.24	7.16	1.06	0.14	0.06	100.18
3(92)	40.56	0.11	11.10	11.61	0.17	19.98	12.24	0.12	0.02	0.06	96.25
13(92)	52.06	0.08	17.34	4.44	0.12	11.29	13.02	1.54	0.06	0.05	100.10
	Ni	Cr	Cu	La	Ce	Nd	Sm	Eu	Tb	Yb	Lu
1(92)	398.6	1617.3	42.1	1.8	5.0	3.0	0.47	0.24	0.1	0.50	0.08
3(92)	512.8	1219.8	1.7	0.5	2	1	0.37	0.13	0.1	0.24	0.04
13(92)	165.8	459.7	6.4	0.5	2	1	0.22	0.16	0.1	0.23	0.03

Concentrations are reported in wt.% (major element as oxides) and ppm (trace elements)

third, to fine-grained gabbronorite. The Σ*REE* patterns of both lithologies show only a gently descending slope (Fig. 11), and chondrite-normalized concentrations are not above eight times chondrite.

CONSTRAINTS ON CONDITIONS OF ALTERATION

The strongly metamorphosed lithologies of the Lukkulaisvaara complex exhibit the highest concentrations of PGE. Thus the crystallization of the ore minerals together with secondary minerals indicate that crystallization of platinum-group minerals and Cu–Ni–Fe sulfides took place under the same conditions as those for the formation of secondary minerals.

Fluid inclusions in epigenetic quartz from gabbroic pegmatites

Fluid inclusions were studied in quartz from quartz veins (two samples), segregations of alteration minerals with sulfides (one sample) and from gabbroic pegmatites (two samples). The rim of quartz grains from gabbroic pegmatites was extensively deformed and cut by thin cracks filled with alteration minerals. Quartz from all samples contains abundant trails of fluid inclusions and clustered zones. Isolated inclusions are rare. The size and composition of the inclusions from the cluster zone and in some trails are highly variable. The diameter of the inclusions varies from 25 μm to less than 1 μm. Small inclusions are typical of quartz grains from gabbroic pegmatites. Most of the inclusions are either monophase or consist of two phases, liquid and vapor. Inclusions filled only by H_2O (initial ice-melting temperatures 0°C and –1°C) usually occur along thin cracks in quartz and in intergranular spaces. We suggest that inclusions of this type were trapped after the crystallization of quartz grains as a result of their alteration. In some cases, hydrocarbon inclusions cut the quartz crystals where aqueous fluid–vapor and aqueous fluid–salt inclusions occur. A few large irregular inclusions contain a solid phase (salt) and vapor. Inclusions of the last three types were examined. Initial ice-melting temperatures between –20°C and –21°C suggest that some H_2O-rich inclusions and inclusions with a solid phase can be modeled in the H_2O–NaCl system. The final melting temperature of ice is in the range –4°C to –0.5°C, which restricts the salinity of the inclusions to 1.0 to 5.0 wt% NaCl equivalent for the H_2O–NaCl system. The volume percent of vapor in all the inclusions at room temperature is much less than that of the liquid or the cubic solid phase. Another type of two-phase CO_2 inclusion (T_{melt} =56.6°C and T_h in the range 10–28°C, and densities between 0.66 and 0.87) is widespread in quartz of quartz veins and gabbroic pegmatites. Inclusions with T_{melt} = 58°C contain CH_4 and N_2. Thus, seven types of fluid inclusion were found, of which the first three predominate: 1) H_2O-rich, 2) CO_2-rich, 3) H_2O–salt, 4) CO_2–H_2O mixture, 5) H_2O–NaCl (solid)–vapor, 6) CH_4–N_2, 7) CO_2–CH_4–N_2.

Determination of the composition of inclusions in quartz from segregations of alteration minerals with sulfides by mass thermography has shown that the inclusions with a decrepitation temperature of about 150°C are filled only with H_2O, whereas inclusions with a decrepitation temperature of 300° to 400°C consist, in general (mol.%), of 63.5% H_2O, 17% CO_2, 1% CH_4, 7% CO, and total sum of hydrocarbon = 11.5%. Inclusions with a decrepitation temperature of up to 550°C, as in the case of the first temperature interval, consist only of H_2O. Determination of the composition of in-

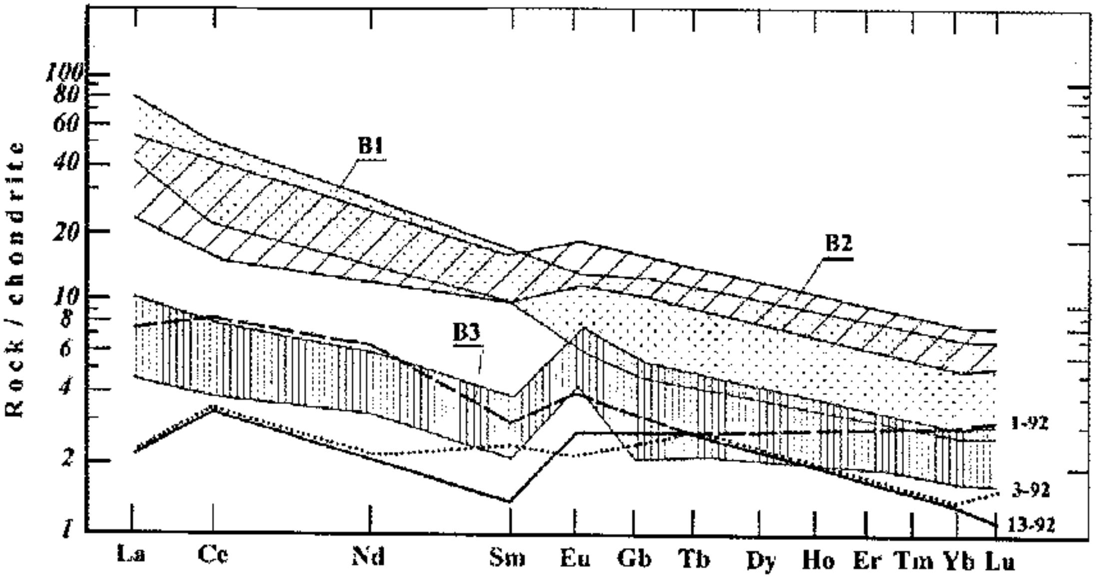

FIG. 11. Chondrite-normalized concentrations of the rare-earth elements in three samples (1–92, 3–92, 13–92) of the fine-grained rocks. B1, B2, B3: Chondrite-normalized data for three suites comprising the marginal suite of sills to the Bushveld Complex (after Hatton & Sharp 1989).

clusions in quartz from the quartz veins provides another type of fluid distribution: for the interval from 250°C to 450°C: 78–79% H_2O, 1–2% CO_2, 0–0.5% CH_4, 17–20% CO (in mol%); for the interval 450–600°C: 80–93% H_2O, 0.5–2% CO_2, 0.2–0.5% CH_4, 5–16% CO.

As noted above, two samples of gabbroic pegmatite were examined. Determination of the composition of inclusions in quartz from this type of rock gave a more complicated picture: for the interval 250–500°C: 57–69% H_2O, 2–20% CO_2, 0–0.4% CH_4, 17–29% CO, 0–2% N_2, for the interval 500–700°C: 71–75% H_2O, 4–17% CO_2, 0.4–1% CH_4, 5–20% CO, 0–1,5% N_2, for the interval 700–900°C: 45–72% H_2O, 4–26% CO_2, 0.04–0.08% CH_4, 8–18% CO, for the interval 900–1000°C: 46–53% H_2O, 2–25% CO_2, 20–34% H_2, 6–9% CO (all gas concentrations in mol. %). The high temperature-intervals of decrepitation testify that quartz from the gabbroic pegmatites has fluid inclusions of magmatic stage. The diameter of magmatic inclusions is less than 0.5 μm.

Gas–H_2O inclusions were used to study T_h. The maximum T_h is 370°C (the group of gas–liquid inclusions with gas contents of 40%). Another group of inclusions showed T_h = 290°C (gas–H_2O inclusions with gas contents of 30–35%). Inclusions with T_h = 230°C and lower are predominantly H_2O-filled. Inclusions filled only with hydrocarbon display a statistical relationship with the group of inclusions with T_h = 290°C. The homogenization of a gas bubble to liquid in the liquid–salt inclusions occurs at 230°C, and the salt is dissolved at 360°C. The difference between the homogenization temperatures allows an estimate of fluid pressure during crystallization of the secondary minerals to be made by applying experimental curves, giving an estimate of 1.5–2.0 kbar. The isochors for the CO_2 inclusions in quartz from the quartz veins and the gabbroic pegmatites (densities 0.66–0.87) indicate a similar pressure, about 1.4–2.5 kbar at 200 < T < 400°C, respectively.

Constraints on conditions of alteration on the basis of paragenetic analysis

To estimate P–T parameters of rock alteration, it is necessary to take into consideration that minerals from reaction zones do not form equilibrated parageneses. Therefore, the stability conditions of certain phases only could be estimated. For aluminosilicates (amphibole and plagioclase), which are stable over a wide interval of P and T, it is possible to study only the aluminum-free system $MgO–SiO_2–H_2O$. FeO is excluded from the system because of the absence of reliable thermodynamic parameters of some iron-bearing phases. Equilibria were calculated with GEØCALC and TWEEQU programs (Berman *et al.* 1987, Berman 1988, 1991). The results are presented in Figure 11a. It is obvious that at P = 2.5 kbar, which is determined from the thermobarometric and geochemical data, the first hydrous silicate to appear at T = 800°C is anthophyllite, then talc appears at

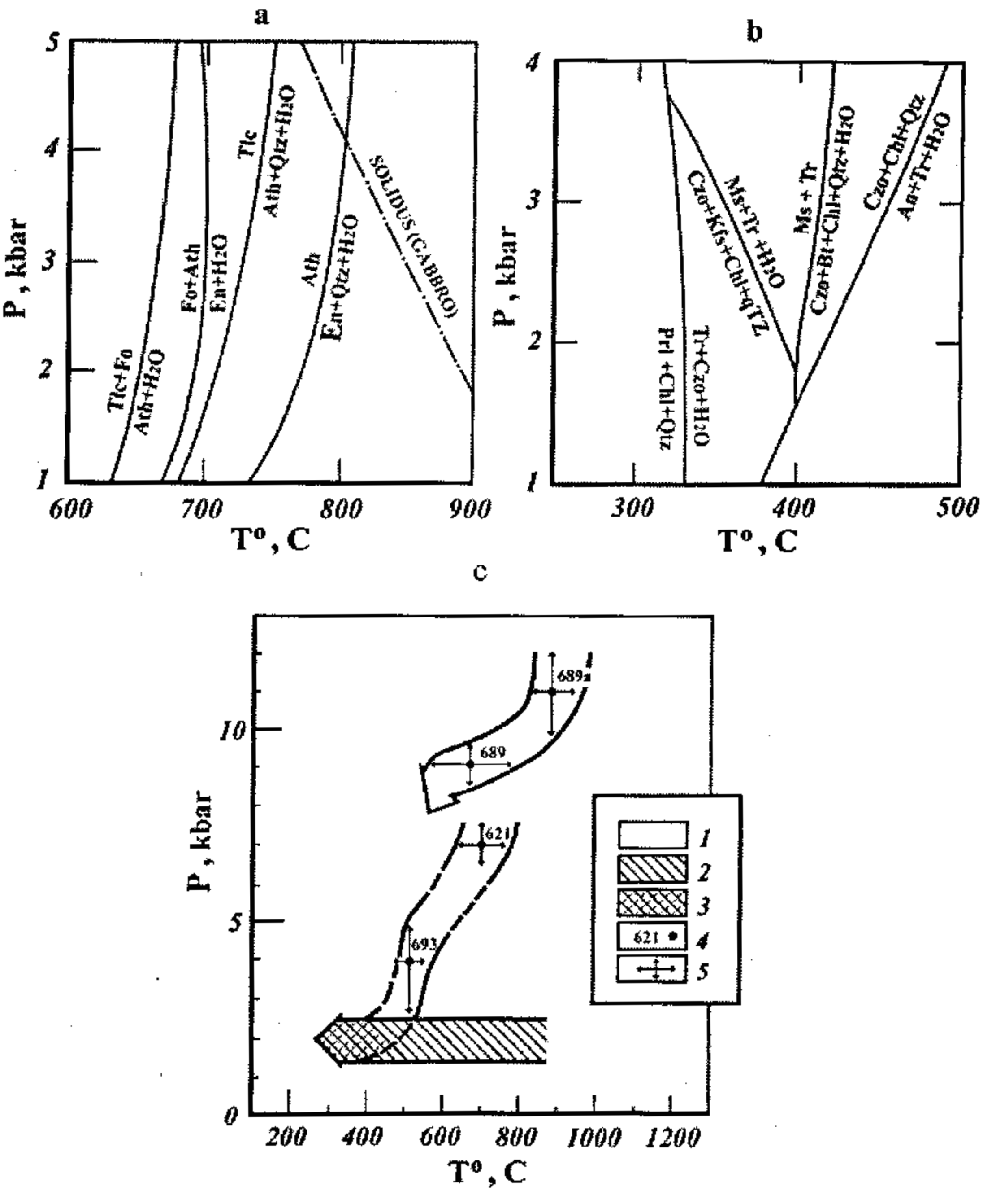

FIG. 12. P–T diagram showing the fields of stability of assemblages of secondary minerals. a. Ore-bearing mineral associations (M1); T in the range 660–800°C, P in the range 1.5–3.0 kbar. b. Ore-bearing mineral associations (M2); T in the range 320–450°C, P in the range 1.5–3.0 kbar. c. Garnet-bearing mineral associations: 1 P–T conditions obtained by TWEEQU method, 2 P–T conditions constraints on the basis of paragenetic analysis, 3 P–T conditions constraints on the basis of an examination of gas–H_2O inclusions, 4 number of the samples, 5 precision of P–T measurements.

$T = 720$°C. The coexistence of these two minerals is possible, and this is a characteristic association in the rocks studied. Enstatite disappears from the system at $T = 700$°C, and anthophyllite does so at $T = 600$°C. Thus, the maximum interval of stability to produce the alteration of the first type of assemblages (M1) is 660–800°C. In reality, this interval is narrower, because some of the equilibria (Fig. 12a) include quartz, but saturation in this system is not reached. At the same time, forsterite, which takes part in other equilibria, is not determined in these rocks. This points to a higher activity of SiO_2 compared to the activity necessary for stability of this mineral.

Estimation of the thermodynamic conditions of stability (P–T parameters) of the M2 assemblages was carried out for the association clinozoisite + tremolite + chlorite + quartz ± biotite ± muscovite (Fig. 12b). The activities of phlogopite in biotite, 0.66, and of clinochlore in chlorite, 0.7, obtained on the basis of mineral compositions (Semenov *et al.* 1997), and models of ideal solid-solution (Koltsov & Rusinova 1997), were taken for calculations. It is obvious that the formation of such an association is possible in the interval 350–450°C, and this temperature interval becomes wider with increasing pressure. The lower limit is 1.5 kbar. The line of univariant equilibrium $Tr + Ms = Czo + Chl + Bt + Qu + H_2O$ at $T = 400$°C divides the field into two parts, low and high temperature, which correspond to the fields of stability of muscovite- and biotite-bearing associations. Pressure and temperature estimations were also obtained using the internally consistent thermodynamic database of Berman *et al.* (1987) and Berman (1988, 1991).

Garnet, hornblende, and plagioclase are the end-member phases used in TWEEQU program calculations (Table 11). There are five possible equilibria that can be written for the selected end-member phases. The results gave $8.5 < P < 12.2$ kbar, $550° < T < 928$°C for a sample taken near the contact with the body of fine-grained rocks, and $6.3 < P < 7.6$ kbar, $625° < T < 755$°C and $2.7 < O < 5.2$ kbar, $480° < T < 550$°C for a sample taken at some distance from the body of fine-grained rocks, the lowest parameters being close to the formation conditions of M2 (a, b) assemblages (Fig. 12c). The equilibria for the garnet, amphibole and plagioclase assemblages of the ore-bearing rocks did not give a precise intersection.

TABLE 11. CHEMICAL COMPOSITION OF GARNET, HORNBLENDE AND PLAGIOCLASE IN HYDROTHERMALLY ALTERED ROCKS, LUKKULAISVAARA INTRUSION

	689a			689			693			621		
	Grt	Hbl	Pl	Grt	Hbl	Pl	Grt	Hbl	Pl	Grt	Hbl	Pl
SiO_2	38.16	39.70	48.60	38.00	41.32	50.08	37.34	42.78	49.66	38.01	40.74	53.37
TiO_2	0.00	0.00	0.00	0.00	0.00	0.00	0.00	0.00	0.00	0.00	0.00	0.00
Al_2O_3	18.16	19.64	29.59	22.10	18.86	31.67	22.05	8.88	31.30	20.09	16.92	28.42
FeO	28.47	16.61	0.00	24.01	10.84	0.00	25.60	9.63	0.46	25.93	21.17	0.97
MnO	2.49	0.00	0.00	1.59	0.00	0.00	2.31	0.00	0.00	6.38	0.00	0.00
MgO	3.61	6.14	0.00	6.45	12.18	0.00	6.07	16.72	0.00	0.98	4.11	0.00
CaO	8.65	13.93	16.41	6.75	19.92	14.81	5.59	11.77	14.69	8.57	12.43	11.94
Na_2O	0.00	2.02	4.35	0.61	2.22	3.34	0.49	1.19	3.40	0.00	0.87	5.04
K_2O	0.00	0.75	0.00	0.00	0.66	0.00	0.00	0.00	0.00	0.00	1.96	0.00

Concentrations reported in wt %.

Three versions of the alteration processes were studied by means of computer modeling using the method of step-by-step multiwave reactor with various values of the water:rock ratio (W/R): 1) bimetasomatic interaction of various minerals, 2) metamorphic alteration, and 3) metasomatic alteration by cooling and decompression during fluid flow. The composition of secondary minerals and the zoning of the rocks with M1 assemblages are well reproduced by a model of diffusive interaction among grains. Minimum W/R values for starting orthopyroxene substitution are 1.5–2.0 orders of magnitude lower than for plagioclase, corresponding to the much wider reaction rims around orthopyroxene grains in these rocks. Na-rich amphibole formed after plagioclase also is characteristic. Integral W/R is near 0.01 and is determined by the fluid reservoir in the remaining melt. The formation of M2 mineral assemblages is described by a metasomatic decompression-process model, development of such a process being favored by low-temperature conditions when brittle deformation led to the formation of fluid conduits.

Sm–Nd AND Rb–Sr ISOTOPE SYSTEMS

Sr and Nd systematics of the main rock-types from the layered series were studied to search for genetic regularities in the spread of isotope signatures across the intrusive body (Amelin & Semenov 1996). The samples analyzed in this study are representative of norite (Lu 603, 606, 623, 860, 302), gabbronorite (Lu 609, 324) and fine-grained norite and gabbronorite (Lu 146/5, 617, 617/1, 854/3, 306/1). Magmatic minerals were separated from fine-grained rocks (Lu 617), and metamorphic minerals were separated from samples of altered sulfide-bearing norite (Lu 302, 860, mineral assemblage M2). The norite sample Lu 302 was taken from near the body of fine-grained rocks (norite II zone, Fig. 3c), and the strongly altered leucocratic norite, sample Lu 860, was taken from the layered series (norite II zone). Separation of the mineral phases was carried out according to standard methods using heavy liquids. Mineral separates were then hand-picked under the microscope. The small size and intergrown nature of the mineral aggregates did not allow separation of a totally pure mineral fraction, and up to 10–20 wt% impurity is present in some separates. The results are presented in Table 12.

The Sm–Nd isochrons were constructed on five whole-rock samples (fine-grained rock) and magmatic mineral phases: 2429 ± 68 Ma, MSWD = 1.66 (whole-

TABLE 12. Sr AND Nd ISOTOPE DATA FOR ROCKS AND MINERAL SEPARATES FROM THE LUKKULAISVAARA LAYERED INTRUSION, NORTHERN KARELIA

Sample	[Sm] ppm	[Nd] ppm	^{147}Sm/ ^{144}Nd	^{143}Nd/ ^{144}Nd ±2σ	ϵ_{Nd} 2440 Ma	T_{DM}	[Rb] ppm	[Sr] ppm	^{87}Rb/ ^{86}Sr	^{87}Sr/ ^{86}Sr ±2σ	I_{Sr} 2440 Ma
fine-grained rocks											
Lu 617	0.440	3.242	0.0823	0.510964±14	+3.27	2525	11.9	190	0.1813	0.705408±18	0.70177
Lu–617 Opx–1	0.504	2.361	0.1294	0.511724±16	+3.32	2569	2.66	283	0.0354	0.703864±16	0.70262
Lu–617 Opx–2	0.124	0.333	0.1608	0.512241±18	+3.56	2610	4.56	179	0.0824	0.704424±19	0.70152
Lu–617 Pl–1	0.316	2.565	0.0746	0.510847±12	+3.39	2514	1.46	422	0.0097	0.703011±14	0.70267
Lu–617 Pl–2	0.191	1.301	0.0891	0.511082±17	+3.43	2520	1.25	478	0.0078	0.702934±12	0.70266
Lu 146/5	0.510	2.008	0.1539	0.512229±16	+3.46	2590	7.09	240	0.0856	0.704608±18	0.70159
Lu–617/1	0.222	0.819	0.1647	0.512279±16	+3.04	2705	0.928	258	0.0104	0.703245±23	0.70288
Lu–308/1	0.451	1.701	0.1610	0.512264±16	+3.94	2556	20.5	337	0.1761	0.707736±23	0.70153
Lu–854/3	0.858	3.831	0.1358	0.511840±12	+3.57	2555	8.37	243	0.0994	0.705114±25	0.70161
mafic rocks from the layered series											
Lu 307	0.932	4.112	0.1374	0.511483±14	−3.95	3312	34.5	286	0.3490	0.710089±16	0.69779
Lu–609	0.616	2.590	0.1443	0.511716±15	−1.54	3152	2.74	234	0.0339	0.703675±14	0.70248
Lu–606	1.067	5.248	0.1230	0.511334±16	−2.34	3038	9.34	265	0.1021	0.705879±29	0.70228
Lu–603	0.853	4.053	0.1277	0.511330±19	−3.88	3206	15.7	254	0.1784	0.707187±16	0.70090
Lu–324	0.451	1.610	0.1703	0.512175±18	−0.74	3405	7.93	274	0.0838	0.704511±25	0.70156
Lu–623	0.485	2.347	0.1252	0.511369±16	−2.35	3056	14.9	337	0.1276	0.706324±14	0.70183
Lu–860	1.911	10.50	0.1105	0.511140±14	−2.17	2952	1.03	514	0.0058	0.705253±13	0.70505
Lu–860 Scp	0.052	0.251	0.1250	0.511355±23	−2.53	3067	1.96	599	0.0090	0.705734±31	0.70542
Lu–149	0.247	1.057	0.1413	0.511679±15	−1.3	3082	2.15	257	0.0243	0.70399±1	0.70313
Lu 149 Pl	0.081	0.589	0.0832	0.510750±35	−1.2	2790	1.25	431	0.0084	0.70308±1	0.70278
Lu–146-7Pl	0.100	0.814	0.0746	0.510591±13	1.6	2790	2.45	402	0.0176	0.70346±1	0.70284
Lu–305–1 Pl	0.224	1.635	0.0830	0.510695±27	−2.2	2849	2.62	461	0.0164	0.70359±1	0.70301
Lu–614 Pl	0.119	1.012	0.0710	0.510525±18	−1.8	2790	12.9	352	0.1058	0.70473±1	0.70100
Secondary minerals (sample Lu–302)											
WR	1.43	7.26	0.1196	0.511467±7	−1.36	2715	37.2	370	0.2904	0.707123±27	0.69689
Chl	0.518	2.69	0.1166	0.511406±15	−1.11	2726	19.9	94.8	0.6089	0.710655±20	0.68919
Czo	2.71	12.9	0.1269	0.511502±11	0.26	2881	21.0	795	0.0765	0.704766±13	0.70207
Pl	0.987	6.13	0.0977	0.511061±11	+0.30	2733	33.3	713	0.1348	0.705882±14	0.70113
Amp	1.53	5.18	0.1787	0.512218±25	−2.56	4034	94.3	34.6	7.8999	0.714524±13	0.43601
Ap	68.3	333	0.1245	0.511386±6	−1.78	2999	9.43	565	0.0482	0.704349±22	0.70265

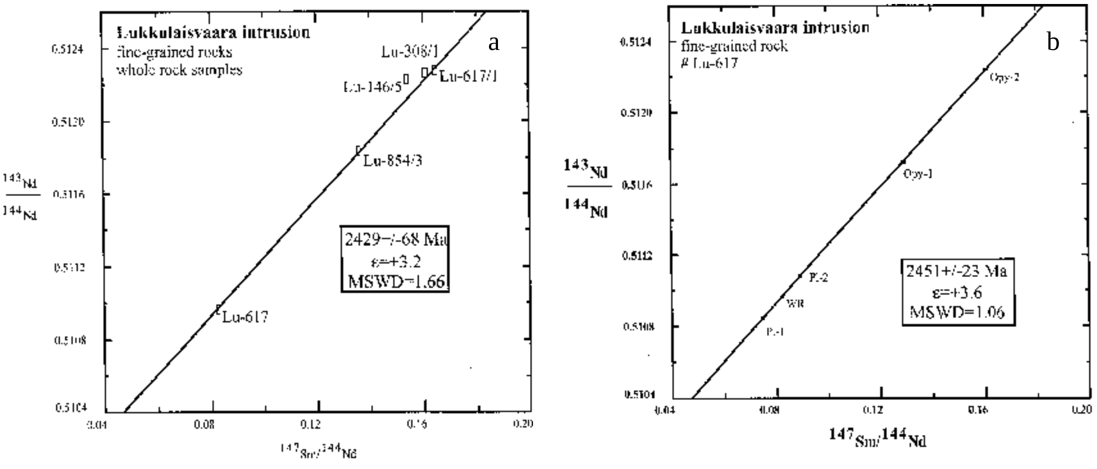

FIG. 13. Sm–Nd isochron diagram for whole-rock samples consisting of fine-grained rocks (a) and magmatic mineral separates from fine-grained norites (b) of the Lukkulaisvaara complex.

rock isochron) and 2451 ± 23 Ma, MSWD = 1.06 (mineral isochron). These estimates are within the error limits of the age obtained by the U–Pb method (2442.1 ± 1.4 Ma, Amelin *et al.* 1995) for the Lukkulaisvaara intrusion (Figs.13a, b).

The calculated values of ε_{Nd} (2440 Ma) determined on a small number of samples display some variations across the section (Fig. 14). Nevertheless, two parts of the section are distinctly characterized by positive values, $\varepsilon_{Nd}(T)$ = +3.04 and +3.94. The most pronounced spike in the Nd isotopic composition is represented by the fine-grained gabbronorite and norite that form sill-like bodies among the rocks of the layered series. At the same time, the rocks of layered series have negative values of $\varepsilon_{Nd}(T)$, from –0.74 to –3.95 (Table 12). However, the Nd content in whole-rock samples varies between 1.6 and 5.2 ppm (with the exception of sample Lu–860, with 10.5 ppm Nd), but no relationships between concentration and neodymium isotope composition are observed. Therefore, these Nd isotopic compositions could be ascribed to initial Nd signatures from the time of emplacement. Such $\varepsilon_{Nd}(T)$ values in the Lukkulaisvaara intrusion could reflect the initial isotopic heterogeneity due to multiple injections of magma. It is noteworthy that there is a tendency for the Nd content to increase (Fig. 14) from the top of the section (gabbronorite II zone, 1.61 ppm) to the bottom (norite I zone, 5.25 ppm).

The values of initial strontium composition in the rocks of the layered series and fine-grained rocks, $I_{sr}(T)$, are within 0.69779 – 0.70505 and 0.70152 – 0.70288, respectively (Table 12). The higher $I_{sr}(T)$ is observed in a sample of strongly metamorphosed leucocratic gabbronorite (Lu 860). Unusually low values of $I_{sr}(T)$ in the range 0.69779–0.69689, were calculated for altered gabbronorite and norite (Lu 307, 302), providing evidence on the post-crystallization mobility of Rb and Sr. The higher value of $I_{sr}(T)$, 0.70505, is apparently a result of metamorphic (metasomatic) alteration, particularly addition of Rb. It is clear that $I_{Sr}(T)$ values obtained for samples Lu 617, 308/1, 603, 606, 623, 307 also suggest that the Rb–Sr system was disturbed, probably because of Rb mobility during metamorphism. The apparent Rb–Sr isochron age for samples Lu 603, 606,

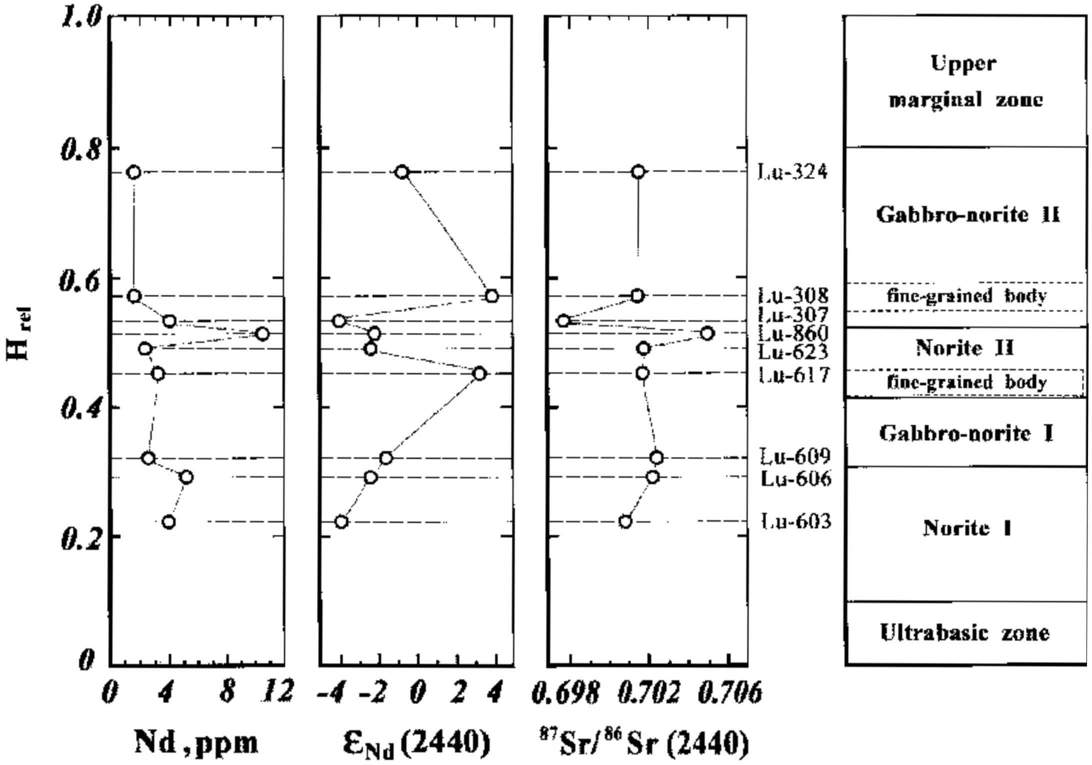

FIG. 14. Initial ε_{Nd} and $^{87}Sr/^{86}Sr$ and Nd concentrations in the Lukkulaisvaara intrusion, plotted against stratigraphic position in the general cross-section. The samples represent all zones of the Lukkulaisvaara intrusion.

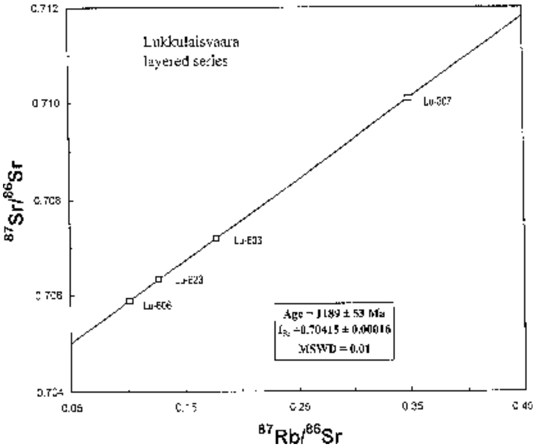

FIG. 15. Rb–Sr isochron diagram for whole-rock samples from layered series of Lukkulaisvaara intrusion.

623, 307, 1189 ± 53 Ma, (Fig. 15) is significantly lower than the age of crystallization, and confirms the opinion that the intrusion was affected by metamorphism.

The Sr and Nd isotope systems of the metamorphic (metasomatic) mineral phases were investigated to determine the time of secondary mineral formation and the source of the fluid. The results of isotope investigations are shown in Table 12.

If the secondary mineral associations had been formed in an open (metasomatic) system, element migration might have occurred and thus affected the isotope dating. Nevertheless, under certain conditions (intense circulation of fluid, considerable amount of fluid, long-lived system) isotope homogeneity of the system can be realized at the local level. In this case, it is possible to obtain meaningful data, suggesting that all selected minerals belong to the simultaneously formed mineral assemblage. The results of the geochronological studies of the minerals from the M2 assemblages prove the multiple origin of the minerals because all the minerals do not form a common trend in Sm–Nd isotope space (Semenov *et al.* 1998). Nevertheless, the age of mineral formation coincides (Semenov *et al.* 1998) with the age of formation of the layered intrusion itself (2442 ± 1.4 Ma, Amelin *et al.* 1995). The metasomatic fluid had more mantle-related characteristics ($\varepsilon_{\mathrm{Nd}}$ from +1.36 to –2.56 for secondary minerals) than the source of the rocks of the layered series ($\varepsilon_{\mathrm{Nd}}$ from –1.9 to –2.4). This could have resulted from different proportions of uplifted material and, consequently, different degrees of contamination of the initial substances by the material of the host rocks.

The apparent Rb–Sr isochron age (782 ± 23 Ma) for the secondary minerals (sample Lu 302) is significantly younger than the age of crystallization, and confirms the opinion that the intrusion was repeatedly affected by metamorphism. The partial re-equilibration of the Rb–Sr isotope system can be related to hydrothermal activity associated with the metamorphic processes. However, apatite is characterized by a low content of Rb and a high content of Sr, so there is little possibility that the initial $^{87}Sr/^{86}Sr$ ratio in apatite has been changed during hydrothermal alteration. Thus, the $^{87}Sr/^{86}Sr = 0.7028$ obtained from apatite was used to calculate the initial Sr composition of the fluid.

DISCUSSION

For the first time, the inner structure of the Lukkulaisvaara intrusion is described in detail, and the evolution of the rock composition is characterized numerically. The massif is shown to be a typical intrusion that differentiated *in situ*. Originally, the southern and northern boundaries of the intrusion were considered its lower and upper contacts, respectively. The primary role of fractional crystallization is confirmed by the vertical sequence of cumulate parageneses and the regularities in the evolution of trace-element concentrations in the rocks and residual magmas.

A comparison of the weighted mean composition of the intrusion with compositionally different magmas (Cameron *et al.* 1979, Hickey & Frey 1982, Dobretsov *et al.* 1980, Bogatikov *et al.* 1987) points to a consistency with magmas of the boninite – marianite series. However, this does not solve the problem concerning the composition of the parental magma because of the possible multiphase structure of the intrusion.

Structures (Fig. 3) similar in morphology to the “potholes” of the Merensky Reef in the Bushveld Complex occur (Campbell *et al.* 1983, Buntin *et al.* 1985, Kruger & Marsh 1985, Campbell 1986, Ballhaus 1988). Many authors (Campbell *et al.* 1983, Campbell 1986, Kruger & Marsh 1985) related the origin of such potholes to injection of new portions of magma. The identical nature of the structures is emphasized by similar host-rocks, namely, spotted anorthosites, gabbroic pegmatites, and poikilitic bronzitites and norites. The presence of fine-grained rocks is a peculiarity of the potholes of the Lukkulaisvaara intrusion. The texture of these rocks suggests rapid crystallization of the newly injected melts.

Fine-grained gabbronorite and norite form large and small lenticular bodies. The weighted mean composition of the Lukkulaisvaara intrusion is chemically close to the weighted mean composition of the large lenticular bodies of fine-grained rocks. We infer this similarity from the closeness of compositions of the petrochemical types of rocks (Fig. 5). Concentrations of Cr are above 300 and 800 ppm, respectively, which is typical for primitive mantle-derived melts. The Σ*REE* concentrations in the fine-grained rocks also have a primitive character, and the patterns are subhorizontal with a slight enrichment in Σ*REE*, up to eight times chondritic.

The distribution of the major elements, Cr, and Ni along the profile through the bodies of fine-grained rock characterizes the latter as independent magmatic formations, the crystallization of which took place under closed-system conditions. Isotopic investigations also support this conclusion.

No mixing or only limited mixing seems to have occurred, since: (1) there is a difference in the physical properties of new and resident melts, (2) the fine-grained rocks are distinctly characterized by positive ε_{Nd}(T) from +3.04 to +3.94, (3) the fine-grained rocks have a primary composition and chilled structure. The temperature of liquidus and densities of the evolved residual melt and the added melt for dry conditions are as follows: 1200°C and 2.70–2.74 g/cm^3 for resident melt; 1280–1300°C and 2.69–2.71 g/cm^3 for the injected melt (Semenov *et al.* 1996). The injection of melt into the chamber suggests that the melt was under higher pressure (P_m, including the partial pressure of the fluid for the "wet" system) than the pressure in the magma chamber. That is why the rapid crystallization of the fine-grained rocks could be due to rapid loss of volatiles (decompression effect) and the difference in temperature.

P–T conditions of metamorphism derived from garnet assosiations (hornblende + garnet + plagioclase) may be a result of additional injection of fresh magma into the crystallized (solidified) part of the chamber (Fig. 3). The maximum pressure (P_m = 12 kbar) obtained from the exocontact zone of the fine-grained rock bodies must correspond to the conditions of intrusion of fresh magma, but the minimum pressure ($P_m = 8 \longrightarrow 4$ kbar) may be connected with the distance of the sample from the site of injection of new magma or with the relaxation of P_m. During the cooling stage, T = 800–900°C reflects the closure temperature of the solidified part of the layered intrusion.

All these data provide evidence of the multiphase nature of the intrusive body. The formation of potholes is connected with these additional intrusions. The composition of magmas injected late is close to that of the primary magma and does not influence the estimated composition of the primary magma.

The results of the present study of the Lukkulaisvaara ore-bearing rocks are summarized as follows: a) discovery of the relations between the Pt-rich ore deposits and altered rocks of the pothole structures. We propose that the potholes play the role of "traps" or act as a geochemical buffer for highly mineralized fluid; b) coexistence of sulfide and precious metal minerals with secondary silicate minerals and calcite in all cases studied; c) the conditions of formation of the ore-bearing mineral associations are: $660 < T < 800$°C and $1.5 < P < 3.0$ kbar (assemblages M1); $320 < T < 450$°C and $1.5 < P < 2.5$ kbar (assemblages M2); d) $800 < T < 900$°C and $8.0 < P < 12.0$ kbar was obtained for the garnet-bearing assemblage M2,d, and $8.0 < P_m < 12.0$ kbar is related to the pressure of a new injection of magma; e) the fluid of the ore-bearing rocks was enriched in chlorine; f) the M1 association developed in veins in pyroxenite and gabbronorite, and the M2 association developed in leucocratic gabbronorite – anorthosites overlying the microgabbronorite of the norite-II zone, are characterized by the richest sulfide and platinum mineralization (Table 1, 2, 3).

Theoretically, it has been proved that the bodies of fine-grained rocks should cause deformation of the host rocks during cooling of the intrusion. Such a deformation caused local decompression, which in turn increased the porosity of the rock and might have acted like a "pump" for the fluid (Zilbershtein *et al.* 1999). The formation of the ore-bearing mineral assemblages (M2) near the contact of large bodies of fine-grained rocks with the underlying rocks was the result of local decompression.

The models of ore-mineral redeposition discussed by Ballhaus & Stumpfl (1986), and Boudreau & McCallum (1992) deal with high-temperature metasomatic alteration by fluid at about 730°C and >1000°C, respectively. The source of this fluid, as proposed by Boudreau & McCallum (1992), could be the intercumulus liquid. Within the Lukkulaisvaara massif, the redeposition of the precious metals took place at temperatures of 660–880°C (M1) and 320–450°C (M2). Isotope data also show that the age of the secondary mineral associations does not differ (within the uncertainties) from the age of the intrusion itself, and that the metasomatic fluid exhibits mantle characteristics. These findings may be the result of a restricted amount of fluid contamination.

CONCLUSIONS

1. The Lukkulaisvaara Layered pluton is a typical *in situ* differentiated intrusion. The weighted mean composition of the intrusion corresponds to a boninitic–marianitic magma. This conclusion does not contradict the idea of the multiphase character of the intrusion because the additional intrusive phases had compositions close to that of the primary magma. Isotopic signatures (ε_{Nd} in the range –0.7 to –3.9 for rocks of the layered series, ε_{Nd} in the range +3.0 to +3.9 for fine-grained rocks) prove the absence of cross-contamination of the primary and additional magmas.

2. Structures similar in morphology to the Merensky Reef structures known as "potholes" were found in the Lukkulaisvaara intrusion. A peculiarity of the potholes here is the presence of fine-grained rocks whose origin could be explained by injections of new magma or melt portions. The texture of these rocks suggests rapid crystallization of the melts, which could be due to rapid loss of volatiles (decompression effect) and to the temperature difference between residual and injected melts. At least some portions of the new magmas were trapped in the solidified part of the intrusive. The injection of new magma took place at a pressure between 9.0 and 11.5 kbar.

3. The richest Fe–Ni–Cu sulfide and PGE mineralization is related to the potholes. The composition of the secondary minerals and the zoning of the ore-bearing rocks with M1 assemblages are well reproduced by a model of the diffusive interaction along grain boundaries. Formation of ore-bearing M2 mineral assemblages took place according to a decompression-induced metasomatic process.

4. The formation of ore-bearing mineral associations occurred at $660 < T < 800°C$, $1.5 < P < 3.0$ kbar (associations M1) and $320 < T < 450°C$, $1.5 < P < 3.0$ kbar (associations M2). Ore-bearing rocks were formed under the influence of highly mineralized reducing hydrothermal solutions 2442 Ma ago by the reworking of the intrusive rocks and an influx of a new portion of the mantle-derived fluid with an εNd value of +2.1 and an initial ^{87}Sr/^{86}Sr of 0.7028.

Acknowledgements

We thank C.J. Stanley, Tuomo T. Alapieti, E.V. Sharkov and A.Y. Barkov. Their critical comments on the earlier versions of the manuscript helped to improve the paper. The work was supported by a grant of the Russian Academy of Sciences for advanced sutdies.

References

Alapieti, T. (1982): The Koillismaa layered igneous complex, Finland – its structure, mineralogy and geochemistry, with emphasis on the distribution of chromium. *Geol. Surv. Finland, Bull.* **319**.

Amelin, Yu.V., Heaman, L.M. & Semenov, V.S. (1995): U–Pb geochronology of layered mafic intrusions in the eastern Baltic Shield: implications for the timing and duration of Paleoproterozoic continental rifting. *Precamb. Res.* **75**, 31- 46.

________ & Semenov, V.S. (1996): Nd and Sr isotopic geochemistry of mafic layered intrusions in the eastern Baltic shield: implications for the evolution of Paleoproterozoic continental mafic magmas. *Contrib. Mineral. Petrol.* **124**, 255-272.

Ballhaus, C.G. (1988): Potholes of the Merensky Reef at Brakspruit Shaft, Rustenburg Platinum Mines: primary disturbances in the magmatic stratigraphy. *Econ. Geol.* **83**, 1140-1158.

________ & Stumpfl, E.F. (1986): Sulfide and platinum mineralization in the Merensky Reef: evidence from hydrous silicates and fluid inclusions. *Contrib. Mineral. Petrol.* **94**, 193-204.

Barkov, A.Y., Gannibal, L.F., Ryungenen, G.I. & Balashov, Yu.A. (1991): U–Pb dating of zircons from the Kivakka layered intruzion, northern Karelia. *Proc. All-Union Seminar* (*St.-Petersburg*), 21- 23 (in Russ.).

________, Martin, R.F., Laajoki, K.V.O., Alapieti, T.T. & Iljina, M.J. (1999): Paragenesis and origin of staurolite from a palladium-rich gabbronorite: an unusual occurence from the Lukkulaisvaara layered intrusion, Russian Karelia. *Neues Jarhb. Mineral., Abh.* **175**, 191-222.

________, Men'shikov, Yu.P., Begizov, V.D. & Lednev, A.I. (1996): Oulankaite, a new platinum- group mineral from the Lukkulaisvaara layered intrusion, northern Karelia, Russia. *Eur. J. Mineral.* **8**, 311-316.

Berman, R.G. (1988): Internally-consistent thermodynamic data for stoichiometric minerals in the system $Na_2O–K_2O–CaO–MgO–FeO–Fe_2O_3–Al_2O_3–SiO_2–TiO_2–H_2O–CO_2$. *J. Petrol.* **29**, 445-522.

________ (1991): Thermobarometry using multi-equilibrium calculations: a new technique, with petrological applications. *Can. Mineral.* **29**, 833-855.

________, Brown, T.H. & Perkins, E.H. (1987): GEØCALC: software for calculation and display of P–T–X phase diagrams. *Am. Mineral.* **72**, 861-862.

Bogatikov, O.A., Kosarev, L.V. & Sharkov, E.V. (1987): *Average Chemical Compositions of the Magmatic Rocks: Reference Book.* Nauka, Moscow, Russia (in Russ.).

Boudreau, A.E. & McCallum, I.S. (1992): Concentration of platinum-group elements by magmatic fluids in layered intrusions. *Econ. Geol.* **87**, 1830-1848.

Buntin, T.I., Grandstaff, P.E., Ulmer, G.C. & Gold, D.P. (1985): A pilot study of geochemical and redox relationships between potholes and adjacent normal Merensky Reef of the Bushveld Complex. *Econ. Geol.* **83**, 975-987.

Cameron, W.E., Nisbet, E.G. & Dietrich, V.J. (1979): Boninites, komatiites and ophiolite basalts. *Nature* **280**, 550-553.

Campbell, I.H. (1986): A fluid dynamic model for the potholes of the Merensky Reef. *Econ. Geol.* **81**, 1118-1125.

________, Naldrett, A.J. & Barnes, S.J. (1983): A model for the origin of the platinum-rich horizons in the Bushveld and Stillwater complexes. *J. Petrol.* **24**, 133-165.

Dobretsov, I.L., Taraskin, A.Ya., Lavrentiev, Yu.G., Sobolev, N.V., Komatsu, M., Tazaki, K., Ditrikh, F. & Oberkhansli, R. (1980): Volcanic rocks of the marianite–boninite series. *In* Geology of the Philippine Sea Floor (A.V. Peyve, ed.). Nauka, Moscow, Russia (149-179; in Russ.).

Felitsin, S.B., Amelin, Yu.V., Semenov, V.S. & Turchenko, S.I. (1989): Oulanga igneous event in North Karelia 2.4 Ga: layered complex, mafic dyke and volcanics. *Int. Assoc. Volcanol. Chem. Earth's Interior, Gen. Meet.* (*Santa Fe*), (abstr.).

Frenkel, M.Ya., Yaroshevsky, A.A., Ariskin, A.A., Barmina, G.S., Koptev-Dvornikov, E.V. & Kireev, B.S.

(1988): *Dynamics of Chamber Differentiation of Basic Magmas*. Nauka, Moscow, Russia (in Russ.).

________, ________, ________, ________, ________ & ________ (1989): Magma differentiation. *In* Magma–Crust Interactions and Evolution. Theophrastus Publications, Athens, Greece (3-91).

GORBATSCHEV, R., LINDH, A., SOLYOM, Z., LAITAKARI, L., ARO, K., LOBACH-ZHUCHENKO, S.B., MARKOV, M.S., IVLIEV, A.I. & BRYHNI, I. (1987): Mafic dyke swarms of the Baltic Shield. *In* Mafic Dyke Swarms (H.C. Halls & W.F. Fahrig, eds.). *Geol. Assoc. Can., Spec. Pap.* 34, 361-372.

HATTON, C. & SHARPE, M. (1989): Significance and origin of boninite-like rocks associated with the Bushveld Complex. *In* Boninites (A. Crawford, ed.). Cambridge Univ. Press, Cambridge, U.K. (174- 207).

HICKEY, R.L. & FREY, F.A. (1982): Geochemical characteristics of boninite series volcanics: implications for their source. *Geochim. Cosmochim. Acta* **46**, 2099-2115.

KLYUNIN, S.F., GROKHOVSAYA, T.L., ZAKHAROV, A.A. & SOLOV'EVA, T.V. (1994): Geology and platinum potential of the Olanga massifs, northern Karelia. *In* Geology and Genesis of Deposits of Platinum-Group Metals. Nauka, Moscow, Russia (111-126; in Russ.).

KOLTSOV, N.B. & RUSINOVA, O.B. (1997): Conditions and formation model for quartz – biotite – potassium feldspar metasomatites of the Muruntau ore deposit. *Petrology* **1**(1), 101-109.

KRUGER, F.J. & MARSH, J.S. (1985): The mineralogy, petrology and origin of the Merensky cyclic unit in the western Bushveld Complex. *Econ. Geol.* **80**, 958-974.

LAVROV, M.M. (1971): The Olanga Group of intrusions. *In* Geochemistry of Hyperbasites of the Karelia–Kola Region. Nauka, Leningrad, Russia (125-141; in Russ.).

PCHELINTSEVA, N.F. & KOPTEV-DVORNIKOV, E.V. (1993): Concentration of noble metals during crystallization of Kivakka layered intrusion (northern Karelia). *Geokhimiya* **1**, 97-113 (in Russ.).

RICHARD, P., SHIMIZU, N. & ALLÈGRE, C.J. (1976): ^{143}Nd/^{146}Nd a natural tracer: an application to oceanic basalts. *Earth Planet. Sci. Lett.* **31**, 269-278.

RUDASHEVSKY, N.S., YAKOVLEVA, O.A., SEMENOV, V.S. & KOPTEV-DVORNIKOV, E.V. (1991): On the model of formation of Pt–Pd low-sulfide ores in layered ultrabasic-basic intrusions (as exemplified by ores of the Lukkulaisvaara Intrusion, northern Karelia). *Dokl. Akad. Nauk* **319**, 479-482 (in Russ.).

SEMENOV, V.S., BELJATSKY, B.V., BALTIBAEV, S.K., GLEBOVITSKY, V.A., KOLTSOV, A.B. & KOPTEV-DVORNIKOV, E.V. (1998): Fe–Ni–Cu sulfide and platinum mineralization in the Lukkulaisvaara layered mafic intrusion (northern Karelia, Russia). *In* International Platinum (N.P. Laverov & V.V. Distler, eds.). Theophrastus Publications, Athens, Greece (79-91).

________, BELYATSKY, B.V., KOLTSOV, A.B., KOTOV, N.V., YAKOVLEVA, O.A., RUDASHEVSKY, N.V. & PCHELINTSEVA, N.F. (1997): Metasomatites and related PGE mineralization of the Lukkulaisvaara layered complex, Olanga group of intrusions, northern Karelia. *Petrology* **5**(2), 121-140.

________, ________, ________, RUDASHEVSKY, N.S. & PCHELINTSEVA, N.F. (1995b): Ore-bearing metasomatites of the Lukkulaisvaara Layered Complex (Olanga Group of the layered intrusions, north Karelia). *In* Petrology and Metallogeny of Volcanic and Intrusive Rocks of the Midcontinent Rift System (Duluth), 169-170.

________, KOPTEV-DVORNIKOV, E.V., BERKOVSKY, A.N., KIREEV, B.S., PCHELINTSEVA, N.F. & VASIL'EVA, M.O. (1995a): Layered intrusions of troctolite – gabbro – norite, Tsipringa complex, northern Karelia: geologic structure and petrology. *Petrology* **3**(6), 645-668 (in Russ.).

________, SHALAEV, V.S., KOLYCHEV, E.A. & BERKOVSKY, A.N. (1996): The Lukkulaisvaara intrusion – multiphase layered complex. *IGCP Project 336, Symp., Program Abstr.* (*Rovaniemi*), 73- 74.

SHMYGALEV, V.I. (1968): Intrusions of basic and ultrabasic rocks of the Olanga Group. *In* Volcanic and hyperbasic complexes of the Proterozoic of the Karelia (A.N. Bogachev, ed.). *Trans. Inst. Geology* (*Petrozavodsk*) **1**, 209-219 (in Russ.).

SIMUSIKOV, V.P. & PAVLOVA, L.A. (2000): Küstelite: does this mineral really exist? *Zap. Vser. Mineral. Obshchest.* **129**(5), 28-30 (in Russ.).

TURCHENKO, S.I. (1992): Precambrian metallogeny related to tectonics in the eastern part of the Baltic Shield. *Precamb. Res.* **58**, 121-141.

________, SEMENOV, V.S., AMELIN, YU.V., LEVCHENKOV, O.A., NEYMARK, L.A., BUIKO, A.K. & KOPTEV-DVORNIKOV, E.V. (1991): The early Proterozoic riftogenic belt of northern Karelia and associated Cu–Ni, PGE and Cu–Au mineralizations. *Geol. Fören. Stockholm Förhand.* **113**, 70-72.

WARD, T.H., JR. (1963): Hierarchical grouping to optimize an objective function. *Am. Statist. Assoc.* **58**(301), 234-244.

ZILBERSHTEIN, A.K., GLEBOVITSKY, V.A., SEMENOV, V.S. & VELIKOSLAVINSKY, S.D. (1999): Deformation inhomogeneity in magmatic intrusions appearing due to cooling decompression and its influence on fluid distribution. *Dokl. Akad. Nauk* **306**(4), 519-522 (in Russ.).

Received December 10, 1999, revised manuscript accepted November 15, 2000.